SUBSTRUCTURING PRECONDITIONERS FOR MORTAR DISCRETIZATION OF A DEGENERATE EVOLUTION PROBLEM

MICOL PENNACCHIO* AND VALERIA SIMONCINI†

Abstract. In this paper we present new efficient variants of structured preconditioners for algebraic linear systems arising from the mortar discretization of a degenerate parabolic system of equations. The new approaches extend and adapt the idea of substructuring preconditioners to the discretization of a degenerate problem in electrocardiology. A polylogarithmic bound for the condition number of the preconditioned matrix is proved and validated by numerical experiments.

1. Introduction. Mathematical models and numerical simulations play an important role in understanding the bioelectric activity of the heart. The most computationally challenging step in a correct simulation of the whole cardiac excitation process is given by the solution of a degenerate parabolic evolution problem, the so called *bidomain* model [16], which involves different space and time scales. Various numerical methods have been adopted in literature to tackle this problem: non-adaptive and adaptive techniques, conforming and non–conforming domain decomposition methods. Non-adaptive methods use fixed spatial grids and fixed time steps; see, e.g., [15, 18, 26]. The resulting modeling tool is very expensive due to the sharp spatial and temporal resolution limits for the whole computational region. Indeed realistic three dimensional simulations typically yield discrete problems with at least $O(10^7)$ unknowns, and time steps of the order of 10^{-2} milliseconds or less.

When spatial adaptivity is taken into account the computational work is concentrated only in regions of high electrical activity [19]. Fully adaptive numerical methods are a very active research area: a first attempt of both spatial and temporal adaptivity in two dimensions can be found in [9, 30], whereas moderate size three dimensional domains were considered in [10].

Domain decomposition techniques may constitute a valid alternative to solve the bidomain model. However, for three dimensional large scale simulations, conforming domain decomposition methods such as those in [27, 32, 12] can still require the use of some kind of adaptivity.

Non–conforming domain decomposition methods try to combine the advantages of the different methods outlined above. More specifically, here we follow a non–conforming non–overlapping domain decomposition approach based on the Mortar Finite Element Method that allows one to use different methods and/or discretizations in each subdomain. Following an adaptive strategy, refinement can then be carried out within each subdomain independently. Hence the computational work can be concentrated only on subdomains of high electrical activity, i.e. crossed by the cardiac wavefront. Since only *weak* matching conditions between domains need to be imposed, the technologies developed for treating the problem with a single-domain approach can be readily employed without any further adaptation. The numerical technique was first applied to the elliptic bidomain equation for the extracellular potential, while a detailed analysis of the discretization errors was developed in [23]. The idea was then extended to a test case of the full evolution problem modeling the cardiac excitation. The resulting approach was compared to a conforming Finite

*Istituto di Matematica Applicata e Tecnologie Informatiche del C.N.R., via Ferrata, 1 - 27100 Pavia, Italy (micol@imati.cnr.it)

†Dipartimento di Matematica, Università di Bologna, Piazza di Porta S. Donato, 5, I-40127 Bologna, Italy; CIRSA, Ravenna and IMATI-CNR, Pavia, Italy (valeria@dm.unibo.it).

Element scheme, the method primarily used so far. The numerical results reported in [22] show the better computational performance of this non–conforming domain decomposition technique, providing additional motivation for its application to more realistic simulations of the whole myocardial excitation process. A computationally sound extension of this numerical technique to the general case of the degenerate parabolic system of equations needs to address the problem of solving the algebraic linear system stemming from the mortar discretization at each time step.

The main focus of this paper is to provide effective preconditioning techniques for solving this possibly ill-conditioned linear system. The numerical discretization considered in this paper is based on a substructuring strategy proposed in [6] for conforming domain decomposition and already applied to the mortar method in [1] for the case of first order finite elements. The scheme has then be extended to a general class of discretization spaces in [4, 3]. This consists in considering a suitable splitting of the nonconforming discretization space in terms of "edge" and "vertex" degrees of freedom and then in using a related block-Jacobi type preconditioner. More precisely, it is important to realize that the typical coefficient matrix is not explicitly available for it stems from a Schur complement reduction, and it can only be used through matrix-vector multiplications. This clearly rules out direct methods, as well as classical iterative schemes. On the other hand, the Preconditioned Conjugate Gradient method (PCG) can be effectively used to solve the associated structured linear system.

To conveniently design an inexpensive preconditioner, the edge and vertex blocks should be suitably replaced. For elliptic problems, an efficient approximation of the edge block of the preconditioner was built in [6] by using a norm equivalence for the space $H_{00}^{1/2}$. For parabolic problems, it was shown in [24] that the edge block of the elliptic preconditioner can be approximated by using a non-standard norm on the trace space, yielding a new additional term that can be easily computed. Here we apply this approach to the degenerate parabolic system of equations, thus generalizing the estimates given in [24]. We further improve the efficiency of the algorithm by also using an efficient variant of the vertex block proposed in [3], yielding a cheaper and easier to implement preconditioner. Following the abstract formulation presented in [4, 3] we prove that the condition number of the preconditioned matrix grows at most polylogarithmically with the number of degrees of freedom per subdomain.

Although these recent developments have been fully exploited to derive the new preconditioners, we stress that the special form of the coefficient matrix largely reflects the *degeneracy* of the parabolic system of equations, thus providing significant additional challenges. In particular, the conductivity tensors associated with the cardiac anisotropy play a critical role in the overall performance of the preconditioner, and careful tuning is required to efficiently mimic their behavior in the approximate operator. Moreover, as already observed in [24], the time step parameter is crucial in correctly coupling the preconditioner matrix blocks.

The outline of the paper is as follows. In section 2 we introduce the reaction–diffusion system of equations modeling the cardiac excitation and we recall results of existence and uniqueness for the solution of this system. In section 3 we briefly review the mortar method and its main properties, and we introduce suitable norms for the trace space. The substructuring preconditioner is proposed and studied in section 4. The main theorem of the paper (Theorem 4.2) stating the convergence of the method and the polylogarithmic bound for the condition number of the preconditioned matrix is presented in the same section and it is proved in section 5. Sections 6 and 7 show

the matrix form of the linear system to be solved and the preconditioners considered. Finally, umerical experiments that validate the theory are shown in Section 8.

For convenience, the symbols $\lesssim$, $\gtrsim$ and $\simeq$ will be used in the paper, i.e. $x_1 \lesssim y_1$, $x_2 \gtrsim y_2$ and $x_3 \simeq y_3$ mean that $x_1 \leq c_1 y_1$, $x_2 \geq c_2 y_2$ and $c_3 x_3 \leq y_3 \leq C_3 x_3$ for some constants c_1, c_2, c_3, C_3 independent of the mesh parameters.

2. Mathematical model. The excitation process in the myocardium is a complex phenomenon characterized by rapid ionic fluxes through the cellular membrane separating the intracellular and the interstitial fluid in the myocardium. Accurate simulations of a complete heartbeat, from the excitation to the recovery phase, have to incorporate realistic fiber geometry, anisotropy of cardiac conductivity and detailed membrane properties. A macroscopic model that can account for these features is the bidomain model (see [16]), consisting of a Reaction-Diffusion (R-D) system of equations for the intra- and extracellular potential u^i and u^e, coupled through the transmembrane potential $v := u^i - u^e$. In this model the cardiac muscle is viewed as two superimposed anisotropic continuous media, intra (i) and extracellular (e), occupying the same volume and separated from each other by the cell membrane.

The R-D system governing the cardiac electric activity may be written in various forms involving different combinations of the variables u^i, u^e, v; see, e.g., [17, 26]. Here, we prefer the formulation followed in [13] to prove existence and uniqueness of the solution, i.e. the following degenerate parabolic R-D system in (u^i, u^e):
Given $I_{app} : \Omega\times]0,T[\to \mathbb{R}$ *and* $u_0^i, u_0^e : \Omega \to \mathbb{R}$, *find* $u^i, u^e : \Omega\times]0,T[\to \mathbb{R}$ *and* $v = u_i - u_e$ *such that*:

$$\begin{array}{ll} \partial_t v - \mathrm{div} M_i \nabla u^i + F(v) = I_{app} & \text{in } \Omega_T \\ \partial_t v + \mathrm{div} M_e \nabla u^e + F(v) = I_{app} & \text{in } \Omega_T \\ \mathbf{n}^T M_i \nabla u^i = 0 & \text{in } \Gamma_T \\ \mathbf{n}^T M_e \nabla u^e = 0 & \text{in } \Gamma_T \\ v(x,0) = v_0(x), & x \in \Omega \end{array} \tag{2.1}$$

with $\Omega_T = \Omega \times (0,T)$, Ω modeling the heart tissue, $\Gamma_T = \Gamma \times (0,T)$, $\Gamma = \partial\Omega$, and $F(v)$ describing the flows of ions across the membrane. Since the aim of this work is to test a numerical procedure, for simplicity but without losing generality, here we focus on the FitzHugh-Nagumo model for the membrane kinetic. Thus, $F(v)$ is a cubic polynomial of v: $F(v) = \frac{\chi}{c_m} I(v)$ with

$$I(v) = Gv(1 - v/v_{th})(1 - v/v_p),$$

χ the ratio of the membrane area per unit tissue, c_m the surface capacitance of the membrane, G the maximum membrane conductance per unit area and v_{th}, v_p the threshold and plateau values of v. The realistic setup of the reaction–diffusion system couples it with a system of ODEs for the ionic gating variables and for the ions concentration (see [21] for more details).

The anisotropic properties of the media are modeled by the intra- and extracellular conductivity tensors $M_i = M_i(x)$ and $M_e = M_e(x)$ assumed to be symmetric positive definite matrices, and

$$0 < \lambda^s_{\min} |\boldsymbol{\xi}|^2 \leq \boldsymbol{\xi}^T M_s(\boldsymbol{x}) \boldsymbol{\xi} \leq \lambda^s_{\max} |\boldsymbol{\xi}|^2 \qquad \forall 0 \neq \boldsymbol{\xi} \in \mathbf{R}^3, \boldsymbol{x} \in \Omega \quad s = i, e. \tag{2.2}$$

A distinguishing feature of the bidomain model lies in the structure of the coupling between the intra– and extracellular media. When the degree of anisotropy is different in the two media, we end up with a system that is of degenerate type.

For the rigorous mathematical derivation of the macroscopic bidomain model from the microscopic properties of the tissue see [25], whereas a result of existence and uniqueness for the solution of (2.1) can be found in [13]. More precisely it was shown that, for a more general ionic current $I(v)$, the solution $\mathbf{u} = (u^i, u^e)$ exists, with $u^i, u^e \in L^2(0,T;H^1(\Omega))$, and is uniquely determined up to a family of additive constants $c(t)$.

REMARK 2.1. *If (u^i, u^e) is a solution of (2.1), it is easy to show that (u^i+c, u^e+c) is still a solution, when $c = c(t)$ is an arbitrary family of additive constants. For the uniqueness of the solution we impose that*

$$\int_{\partial\Omega} u^e \, ds = 0. \tag{2.3}$$

2.1. Variational formulation. In order to write problem (2.1) in a compact form we follow the abstract formulation used in [13] to prove existence and uniqueness of the solution. Let Ω be a Lipschitz domain of $\mathbb{R}^2$ and let us assume that $I_{app} \in L^2(\Omega\times]0,T[)$ and $v_0 \in L^2(\Omega)$. We choose as test functions

$$\hat{u}_{i,e} \in H^1(\Omega) \quad \text{with} \quad \hat{v} := \hat{u}^i - \hat{u}^e,$$

and we multiply the two equations of (2.1) by $\hat{u}^i$ and $-\hat{u}^e$ respectively. Summing up them after integration on Ω we get:

$$\int_\Omega \partial_t v \hat{v} \, dx + \sum_{i,e} \int_\Omega \nabla \hat{u}_{i,e}^T M_{i,e} \nabla u_{i,e} \, dx + \int_\Omega F(v)\hat{v} \, dx = \int_\Omega I_{app}\hat{v} \, dx$$

We then define the product space $V = H^1(\Omega) \times H^1(\Omega)$, its closed subspace $\mathcal{V} := \left\{\mathbf{u} \in V \mid \int_{\partial\Omega} u^e \, ds = 0\right\}$, and the norm and seminorm $\|\cdot\|_V, |\cdot|_V$ as

$$\|\mathbf{u}\|_V^2 := |\mathbf{u}|_V^2 + \int_\Omega |u^i - u^e|^2 \, dx, \qquad |\mathbf{u}|_V^2 := \int_\Omega |\nabla u^i|^2 \, dx + \int_\Omega |\nabla u^e|^2 \, dx \tag{2.4}$$

with $\mathbf{u} = (u^i, u^e)^T$. We introduce the following bilinear forms on $\mathcal{V}$:

$$\begin{aligned} a(\mathbf{u}, \hat{\mathbf{u}}) &:= \int_\Omega (\nabla \hat{u}^i)^T M_i \nabla u^i \, dx + \int_\Omega (\nabla \hat{u}^e)^T M_e \nabla u^e \, dx, \\ b(\mathbf{u}, \hat{\mathbf{u}}) &:= \int_\Omega (u^i - u^e)(\hat{u}^i - \hat{u}^e) \, dx. \end{aligned} \tag{2.5}$$

Both forms a and b are continuous, symmetric and nonnegative definite. By using (2.2), it can be easily verified that in $\mathcal{V}$

$$\lambda_{\min}(M_{i,e}) \, |\mathbf{u}|_V^2 \le a(\mathbf{u}, \mathbf{u}) \le \lambda_{\max}(M_{i,e}) \, |\mathbf{u}|_V^2 \,, \tag{2.6}$$

and that the sum $a+b$ is coercive and continuous in $\mathcal{V}$. Finally, we define the functional $g(\hat{\mathbf{u}}) := \int_\Omega I_{app}\hat{v} \, dx$ with $\hat{v} = \hat{u}^i - \hat{u}^e$, and the non-linear form $\mathcal{F}$

$$\mathcal{F}(\mathbf{u}, \hat{\mathbf{u}}) := \int_\Omega F(u^i - u^e)(\hat{u}^i - \hat{u}^e) \, dx. \tag{2.7}$$

The solution $\mathbf{u} :]0,T[\to \mathcal{V}$ of (2.1) thus satisfies the variational evolution equation:

$$\begin{aligned} &\frac{d}{dt} b(\mathbf{u}, \hat{\mathbf{u}}) + a(\mathbf{u}, \hat{\mathbf{u}}) + \mathcal{F}(\mathbf{u}, \hat{\mathbf{u}}) = g(\hat{\mathbf{u}}) \quad \text{in } \mathcal{V}', \quad a.e. \text{ in }]0,T[\\ &b(\mathbf{u}(0), \hat{\mathbf{u}}) = b(\mathbf{u}_0, \hat{\mathbf{u}}). \end{aligned} \tag{2.8}$$

Since the kernel of b has infinite dimension, the differential equation in (2.8) is degenerate; see [13]. Finally, under the assumption that the ionic current model has a cubic growth at infinity, it is shown in [13] that a strong solution $\mathbf{u} = (u^i, u^e)$ exists and $u^i, u^e \in L^2(0,T;H^2(\Omega))$.

3. Mortar Method. We now recall the mortar method, its main properties and we apply it to the cardiac R-D problem (2.1). We follow the notation used in [5], then let Ω be a bounded polygonal domain of $\mathbb{R}^2$ representing the cardiac tissue and let $\{\Omega_\ell\}_{l=1}^L$ be a partition of Ω into L non–overlapping subdomains Ω_ℓ:

$$\Omega = \cup_{\ell=1}^L \Omega_\ell \qquad \text{where} \qquad \Omega_k \cap \Omega_\ell = \emptyset \quad \text{if} \quad k \neq \ell.$$

We denote by $\gamma_\ell^{(i)}$ $(i = 1, \ldots, 4)$ the i-th side of the ℓ-domain, so that $\partial\Omega_\ell = \cup_{i=1}^4 \gamma_\ell^{(i)}$, and setting $\Gamma_{\ell k} = \partial\Omega_k \cap \partial\Omega_\ell$ then the so–called skeleton of the decomposition is

$$\mathcal{S} = \cup \Gamma_{\ell k}.$$

Definition 3.1. *We say that a decomposition is* geometrically conforming *if each edge $\gamma_\ell^{(i)}$ coincides with $\Gamma_{\ell n}$ for some n. If the decomposition is not geometrically conforming, then each interior edge $\gamma_\ell^{(i)}$ will be in general split as the union of several segments $\Gamma_{\ell n}$:*

$$\gamma_\ell^{(i)} = \bigcup_{n \in I_\ell^{(i)}} \Gamma_{\ell n}, \qquad \textit{where} \quad I_\ell^{(i)} = \{n : \ |\partial\Omega_n \cap \gamma_\ell^{(i)}| \neq 0\}.$$

We also make the following regularity assumptions on the subdomains Ω_ℓ:

(G1) the subdomains are regular in shape and the geometrical decomposition is graded, that is
(a) there exists a positive constant c_0 such that, for all k, Ω_ℓ contains a ball of diameter $c_0 H_k$, it is contained in a ball of diameter H_k, and the length of each side is bounded from below by $c_0 H_k$; moreover any interior angle ω satisfies $0 < c_1 < \omega < c_2 < \pi$ (c_0, c_1, and c_2 independent of k);
(b) there exists a positive constant c_3 such that, if ℓ, k are such that $|\Gamma_{\ell k} \cap \partial\Omega_\ell| > 0$, then it holds $H_k/H_\ell \leq c_3$;

(G2) the following bound holds $\max_{(\ell,i)} \left(\frac{|\gamma_\ell^{(i)}|}{\min_{n \in I_\ell^{(i)}} |\Gamma_{\ell n}|} \right) \leq \rho$.

The constants appearing in the estimates of the following sections will in general depend on the bound ρ.

The Mortar Method is applied by choosing a splitting of the skeleton $\mathcal{S}$ as the disjoint union of a certain number of subdomain sides $\gamma_\ell^{(i)}$, called *mortar* or *slave* sides: we choose an index set $I \subset \{1, \ldots, L\} \times \{1, \ldots, 4\}$ such that

$$\mathcal{S} = \bigcup_{(\ell,i) \in I} \gamma_\ell^{(i)}.$$

Finally, $I^* \subset \{1, \ldots, L\} \times \{1, \ldots, 4\}$ denotes the index–set corresponding to *trace* or *master* sides, and is defined as

$$I^* \cap I = \emptyset \quad \text{and} \quad \mathcal{S} = \bigcup_{(\ell,i) \in I^*} \gamma_\ell^{(i)}.$$

3.1. Continuous Problem. We next adapt the variational formulation of section 2.1 to the mortar setting. By using the above splitting of the domain, we consider a non–conforming domain decomposition method introducing the following functional spaces

$$W = \prod_{\ell=1}^{L} H^1(\Omega_\ell) \qquad X = \left\{ \mathbf{u} = (u^i, u^e) \in W \times W \mid \int_{\partial\Omega} u^e \, ds = 0 \right\},$$

with the associated broken norm and seminorm:

$$(|\phi|_1^*)^2 = \sum_\ell |\phi|^2_{1,\Omega_\ell}, \qquad (|\boldsymbol{\phi}|_X^*)^2 = \sum_\ell |\phi^i|^2_{1,\Omega_\ell} + \sum_\ell |\phi^e|^2_{1,\Omega_\ell},$$
$$(\|\boldsymbol{\phi}\|_X^*)^2 = \sum_\ell |\phi^i|^2_{1,\Omega_\ell} + \sum_\ell |\phi^e|^2_{1,\Omega_\ell} + \sum_\ell H_\ell^{-2} \int_{\Omega_\ell} |\phi^i - \phi^e|^2 \, dx,$$

where $\boldsymbol{\phi} = (\phi^i, \phi^e)$ and H_ℓ is the diameter of the subdomain Ω_ℓ. We will also use

$$Y = \prod_{\ell=1}^{L} H^{1/2}(\partial\Omega_\ell), \qquad T = \left\{ \boldsymbol{\eta} = (\eta^i, \eta^e) \in Y \times Y \mid \int_{\partial\Omega} \eta^e \, ds = 0 \right\},$$

with norm and seminorm on Y and T defined as:

$$|\phi|_Y^2 = \sum_{l=1} |\phi|^2_{1/2,\partial\Omega_\ell}, \|\phi\|_Y^2 = \sum_{l=1} \|\phi\|^2_{1/2,\partial\Omega_\ell}, \quad |\boldsymbol{\phi}|_T^2 = |\phi^i|_Y^2 + |\phi^e|_Y^2$$
$$\|\boldsymbol{\phi}\|_T^2 = |\phi^i|_Y^2 + |\phi^e|_Y^2 + \sum_\ell H_\ell^{-1} \int_{\partial\Omega_\ell} |\phi^i - \phi^e|^2 \, d\sigma.$$

We remark that the above norms are scaling invariant, that is they are preserved when Ω_ℓ is rescaled to the reference domain $]0,1[^2$.

The bilinear form (2.5) transforms into the composition

$$a_X(\mathbf{u}, \hat{\mathbf{u}}) := a_W^i(u^i, \hat{u}^i) + a_W^e(u^e, \hat{u}^e) \quad \forall\, \mathbf{u}, \hat{\mathbf{u}} \in X, \tag{3.1}$$
$$a_W^s(u^s, \hat{u}^s) := \sum_\ell \int_{\Omega_\ell} (\nabla u_\ell^s)^T M_s \nabla \hat{u}_\ell^s \, dx \quad \forall\, u^s, \hat{u}^s \in W, \quad s = i, e. \tag{3.2}$$

To cope with the lack of coerciveness of a_X and $a_X + b$, we restrict to subspaces of X of functions satisfying a suitable weak continuity constraint. More precisely, for any subspace $M \subset L^2(S)$, let $\mathcal{W}(M)$ and $\mathcal{X}(M)$ be the *constrained* spaces:

$$\mathcal{W}(M) = \left\{ \phi \in W \mid \int_{\mathcal{S}} [\phi] \, \lambda \, ds = 0, \quad \forall \lambda \in M \right\}$$

where $[\phi]$ denotes the jump of ϕ across the skeleton $\mathcal{S}$ and let

$$\mathcal{X}(M) = \left\{ \Phi = (\phi^i, \phi^e) \in \mathcal{W} \times \mathcal{W} \mid \int_{\partial\Omega} \phi^e \, ds = 0 \right\}.$$

Under minimal conditions on M (M must contain the constants on each subdomain edge) the bilinear forms a_X and $a_X + b$ are coercive on $\mathcal{X}(M)$, and in particular, there exist constants $\gamma, \alpha > 0$ such that

$$\alpha \|\mathbf{u}\|_X^2 \le a_X(\mathbf{u}, \mathbf{u}) + b(\mathbf{u}, \mathbf{u}) \le \gamma \|\mathbf{u}\|_X^2 \quad \forall\, \mathbf{u} \in \mathcal{X}. \tag{3.3}$$

In other words, we impose the weak continuity by requiring that the jump of the solution on each side is orthogonal to a multiplier space. We remark that the strong continuity of the solution at the cross points is not required.

We say that $\phi \in W$ satisfies the *mortar condition* on $\mathcal{S}$ if $\phi \in \mathcal{W}(M)$, and for $\Phi = (\phi^i, \phi^e) \in X$ if each component ϕ^i, ϕ^e belongs to $\mathcal{W}(M)$.

Once the multiplier space M has been chosen, the following problem can be formulated:

Problem (P): *find* $\mathbf{u} = (u^i, u^e)$ with $\mathbf{u} :]0, T[\to \mathcal{X}(M)$ such that for all $\hat{\mathbf{u}} \in \mathcal{X}(M)$

$$\begin{aligned} &\frac{d}{dt} b(\mathbf{u}, \hat{\mathbf{u}}) + a_X(\mathbf{u}, \hat{\mathbf{u}}) + \langle \mathcal{F}\mathbf{u}, \hat{\mathbf{u}} \rangle = (I_{app}, \hat{\mathbf{u}}) \\ &b(\mathbf{u}(0), \hat{\mathbf{u}}) = b(\mathbf{u}_0, \hat{\mathbf{u}}). \end{aligned} \tag{3.4}$$

3.2. Time discretization. A semi–implicit scheme is used to discretize (3.4): implicit for the diffusion term and explicit for the reaction term. Let τ be the time step. The time discrete problem reads as:

$$b\left(\frac{\mathbf{u}^{k+1}}{\tau}, \hat{\mathbf{u}}\right) + a_X(\mathbf{u}^{k+1}, \hat{\mathbf{u}}) = -\langle \mathcal{F}\mathbf{u}^k, \hat{\mathbf{u}} \rangle + b\left(\frac{\mathbf{u}^k}{\tau}, \hat{\mathbf{u}}\right) + (I_{app}, \hat{\mathbf{u}}) \tag{3.5}$$

with $\mathbf{u}^0(x,t) = \mathbf{u}_0(x,t)$ and $n = 1, \ldots, N_T$. Let us define

$$\begin{aligned} a_\tau(\mathbf{u}, \Phi) &= b(\mathbf{u}, \hat{\mathbf{u}}) + \tau a_X(\mathbf{u}, \hat{\mathbf{u}}) \\ (g_k, \hat{\mathbf{u}}) &= \tau \left[-\langle \mathcal{F}\mathbf{u}^k, \hat{\mathbf{u}} \rangle + b\left(\mathbf{u}^k, \hat{\mathbf{u}}\right) + (I_{app}, \hat{\mathbf{u}}) \right] \end{aligned} \tag{3.6}$$

and let us drop, for notational convenience, the index k so that $\mathbf{u} = \mathbf{u}^{k+1}$. Then, for each time step, the scheme (3.5) leads to the following problem:

Problem ($\mathbf{P}_\tau$): *find* $\mathbf{u} \in \mathcal{X}$ *such that for all* $\hat{\mathbf{u}} \in \mathcal{X}$*:*

$$a_\tau(\mathbf{u}, \hat{\mathbf{u}}) = (g_k, \hat{\mathbf{u}}). \tag{3.7}$$

Norms on X and T. To deal with Problem ($\mathbf{P}_\tau$) we introduce the following norm defined for all $\mathbf{u} = (u^i, u^e) \in X$:

$$\|\mathbf{u}\|_\tau^2 = \sum_\ell \frac{1}{H_\ell^2} \int_{\Omega_\ell} |u^i - u^e|^2 \, dx + \tau \sum_\ell \left(\int_{\Omega_\ell} |\nabla u^i|^2 \, dx + \int_{\Omega_\ell} |\nabla u^e|^2 \, dx \right). \tag{3.8}$$

Next lemma gives boundedness and positive definiteness of $a_\tau(\cdot, \cdot)$; the proof immediately follows from the boundedness and ellipticity of $a_X(\cdot, \cdot)$.

LEMMA 3.2. *There exist positive constants C and c, independent of τ, such that:*
a) $|a_\tau(\mathbf{u}, \Phi)| \le C \, \|\mathbf{u}\|_\tau \, \|\Phi\|_\tau, \qquad \forall \mathbf{u}, \Phi \in \mathcal{X}$
b) $|a_\tau(\mathbf{u}, \mathbf{u})| \ge c \, \|\mathbf{u}\|_\tau^2, \qquad \forall \mathbf{u} \in \mathcal{X}$

The second norm that we consider on X is the a_τ–norm defined as:

$$\|\mathbf{u}\|_{a_\tau} = \sqrt{a_\tau(\mathbf{u}, \mathbf{u})} \tag{3.9}$$

then, from Lemma 3.2 we get that the a_τ-norm is equivalent to the τ-norm.

Following the theory in [24], we note that the natural norm for elements $\boldsymbol{\eta} = (\eta^i, \eta^e)$ of the trace space T is given by

$$\|\boldsymbol{\eta}\|_{T,a_\tau} := \inf_{\mathbf{u}\in X:\, \mathbf{u}_{|S}=\boldsymbol{\eta}} \|u\|_{a_\tau}. \tag{3.10}$$

As already observed in [24], dealing with (3.10) is not convenient. For this reason, we introduce another equivalent and more accessible norm that also suggests the structure of a possible preconditioner. More specifically, we define:

$$\|\boldsymbol{\eta}\|^2_{T,\tau} := \sum_\ell \left(\frac{\tau^{1/2}}{H_\ell} \|\eta^i_\ell - \eta^e_\ell\|_{0,\Gamma_\ell} + \tau |\eta^i_\ell|^2_{1/2,\Gamma_\ell} + \tau |\eta^e_\ell|^2_{1/2,\Gamma_\ell} \right). \tag{3.11}$$

We next prove the equivalence of these last two norms.

LEMMA 3.3. *The following norm equivalence holds for all $\boldsymbol{\eta} \in T$:*

$$\|\boldsymbol{\eta}\|_{T,a_\tau} \simeq \|\boldsymbol{\eta}\|_{T,\tau}.$$

Proof. We split the proof in two parts. We first prove that $\|\boldsymbol{\eta}\|_{T,\tau} \lesssim \|\boldsymbol{\eta}\|_{T,a_\tau}$, and then we show that $\|\boldsymbol{\eta}\|_{T,a_\tau} \lesssim \|\boldsymbol{\eta}\|_{T,\tau}$.

i) For simplicity we first consider a reference domain $\hat{\Omega}$ of unitary diameter. Setting $\hat{\Gamma} = \partial\hat{\Omega}$, then for all $\phi \in H^1(\hat{\Omega})$ it holds (see [31, 7])

$$\|\phi\|^2_{0,\hat{\Gamma}} \le C \, \|\phi\|_{0,\hat{\Omega}} \, \|\nabla\phi\|_{0,\hat{\Omega}}. \tag{3.12}$$

From (2.6) and the definition of a_τ we have that

$$(|\mathbf{u}|^*_X)^2 \le \frac{1}{\tau\lambda_{min}} a_\tau(\mathbf{u},\mathbf{u}) \tag{3.13}$$

hence, in our case we get:

$$\|\eta^i - \eta^e\|^2_{0,\hat{\Gamma}} \le C \sqrt{b(\mathbf{u},\mathbf{u})} \; \tau^{-1/2} \sqrt{a_\tau(\mathbf{u},\mathbf{u})} \tag{3.14}$$

with $\boldsymbol{\eta} = (\eta^i, \eta^e)$ and $\mathbf{u} = (u^i, u^e)$ such that $\mathbf{u}_{|\hat{\Gamma}} = \boldsymbol{\eta}$. Then

$$\tau^{1/2} \|\eta^i - \eta^e\|^2_{0,\hat{\Gamma}} \lesssim \sqrt{b(\mathbf{u},\mathbf{u})} \, \sqrt{a_\tau(\mathbf{u},\mathbf{u})} \tag{3.15}$$

and thanks to the inequality $ab \le \frac{\delta}{2}a^2 + \frac{1}{2\delta}b^2$ we obtain

$$\tau^{1/2} \|\eta^i - \eta^e\|^2_{0,\hat{\Gamma}} \lesssim b(\mathbf{u},\mathbf{u}) + a_\tau(\mathbf{u},\mathbf{u}). \tag{3.16}$$

By adding $\tau|\eta^i|^2_{1/2,\hat{\Gamma}} + \tau|\eta^e|^2_{1/2,\hat{\Gamma}}$ and using $|\eta^{i,e}|^2_{1/2,\hat{\Gamma}} \lesssim |u_{i,e}|^2_{1,\hat{\Omega}}$ (see [20]), we get:

$$\tau^{1/2} \|\eta^i - \eta^e\|^2_{0,\hat{\Gamma}} + \tau|\eta^i|^2_{1/2,\hat{\Gamma}} + \tau|\eta^e|^2_{1/2,\hat{\Gamma}} \lesssim a_\tau(\mathbf{u},\mathbf{u}).$$

Now let $\boldsymbol{\eta} = (\boldsymbol{\eta}_\ell)_{\ell=1,\dots,L} \in \mathcal{T}$ with $\boldsymbol{\eta}_\ell = (\eta^i_\ell, \eta^e_\ell)$ and let $\mathbf{u} = (\mathbf{u}_\ell)_\ell$ be such that $\mathbf{u}_{|\mathcal{S}} = \boldsymbol{\eta}$, then if we rescale (3.16) to a domain Ω_ℓ of diameter H_ℓ we obtain that

$$H_\ell^{-1} \tau^{1/2} \|\eta^i_\ell - \eta^e_\ell\|^2_{0,\Gamma_\ell} + \tau |\boldsymbol{\eta}_\ell|^2_{1/2,\Gamma_\ell} \lesssim a_\tau(\mathbf{u}_\ell, \mathbf{u}_\ell).$$

The result follows by summing over all subdomains Ω_ℓ.

ii) We next prove that $\|\boldsymbol{\eta}\|_{T,a_\tau} \lesssim \|\boldsymbol{\eta}\|_{T,\tau}$. Let $\boldsymbol{\eta} = (\boldsymbol{\eta}_\ell)_{\ell=1,\dots,L} \in T$. Then we have to build an extension $\mathbf{u}$ of $\boldsymbol{\eta}$ such that $\mathbf{u}_{|\mathcal{S}} = \boldsymbol{\eta}$ and $\|\mathbf{u}\|_{a_\tau} \lesssim \|\boldsymbol{\eta}\|_{T,a_\tau}$.

Again we first focus on a domain $\hat{\Omega}$ of unitary diameter with $\hat{\Gamma} = \partial\hat{\Omega}$. Consider the function $\eta^i - \eta^e$ and the auxiliary problem:

$$\begin{cases} -\tau\Delta w + w = 0 & \in \hat{\Omega} \\ w = \eta^i - \eta^e & \text{on } \hat{\Gamma}. \end{cases} \tag{3.17}$$

Proceeding as in the case of one parabolic equation [24] yields

$$\|w\|^2_{0,\hat{\Omega}} + \tau\,|w|^2_{1,\hat{\Omega}} \lesssim \tau^{1/2}\|\eta^i - \eta^e\|^2_{0,\hat{\Gamma}} + \tau\left|\eta^i - \eta^e\right|^2_{1/2,\hat{\Gamma}}. \tag{3.18}$$

Consider the function $\eta^i + \eta^e$ and the problem

$$\begin{cases} -\Delta z = 0 & \in \hat{\Omega} \\ z = \eta^i + \eta^e & \text{on } \hat{\Gamma}. \end{cases} \tag{3.19}$$

By using standard arguments, it follows that (3.19) admits a solution z satisfying the estimate:

$$|z|^2_{1,\hat{\Omega}} \lesssim \left|\eta^i + \eta^e\right|^2_{1/2,\hat{\Gamma}}. \tag{3.20}$$

By taking $u^i = (w+z)/2$ and $u^e = (z-w)/2$, there exists $\mathbf{u} = (u^i, u^e)$ such that $\mathbf{u}_{|\hat{\Gamma}} = \boldsymbol{\eta}$ and

$$\|u^i - u^e\|^2_{0,\hat{\Omega}} + \tau\left|u^i\right|^2_{1,\hat{\Omega}} + \tau\,|u^e|^2_{1,\hat{\Omega}} \lesssim \tau^{1/2}\|\eta^i - \eta^e\|^2_{0,\hat{\Gamma}} + \tau\left|\eta^i\right|^2_{1/2,\hat{\Gamma}} + \tau\,|\eta^e|^2_{1/2,\hat{\Gamma}}.$$

The result follows from summing over all subdomains Ω_ℓ with diameter H_ℓ. □

3.3. Discrete Mortar Problem. To obtain a fully discrete problem, we discretize (3.7) in space by introducing, for each subdomain Ω_ℓ, a family $\mathcal{V}_h^\ell$ of finite dimensional subspaces of $H^1(\Omega_\ell) \cap C^0(\bar{\Omega}_\ell)$ satisfying condition (2.3).

Let $Y_h^\ell = \mathcal{V}^\ell_{h|\partial\Omega_\ell}$ and, for any $\gamma_\ell^{(i)}$ of the subdomains Ω_ℓ, let

$$Y_{\ell,i} := \left\{\eta \,:\, \eta \text{ is the trace on } \gamma_\ell^{(i)} \text{ of some } u_\ell \in \mathcal{V}_h^\ell\right\} \tag{3.21}$$

$$Y^0_{\ell,i} := \left\{\eta \in Y_{\ell,i};\, \eta = 0 \text{ at the vertices of } \gamma_\ell^{(i)}\right\} \tag{3.22}$$

$$T_{\ell,i} := Y_{\ell,i} \times Y_{\ell,i} \qquad T^0_{\ell,i} := Y^0_{\ell,i} \times Y^0_{\ell,i}. \tag{3.23}$$

We set

$$W_h = \prod_{\ell=1}^{L} \mathcal{V}_h^\ell \subset W, \qquad X_h = W_h \times W_h \subset X$$

$$Y_h = \prod_{\ell=1}^{L} Y_h^\ell \subset Y, \qquad T_h = Y_h \times Y_h \subset T.$$

Given a finite dimensional multiplier space $M_h \subset L^2(S)$, we can introduce the constrained approximation and trace spaces $\mathcal{X}_h$ and $\mathcal{Y}_h$ as follows

$$\mathcal{W}_h = \left\{\phi_h \in W_h,\ \int_{\mathcal{S}} [\phi_h]\ \lambda\ ds = 0, \quad \forall \lambda \in M_h\right\} \qquad \mathcal{X}_h = \mathcal{W}_h \times \mathcal{W}_h$$

$$\mathcal{Y}_h = \left\{\eta \in Y_h,\ \int_{\mathcal{S}} [\eta]\ \lambda\ ds = 0, \quad \forall \lambda \in M_h\right\} \qquad \mathcal{T}_h = \mathcal{Y}_h \times \mathcal{Y}_h.$$

Moreover we denote by $\mathcal{V}_h^{\ell,0} \subset \mathcal{V}_h^\ell$ and $\mathcal{X}_h^0 \subset \mathcal{X}$ the subspaces of functions vanishing on the skeleton. Remark that elements of $\mathcal{X}_h^0$ have null jump, trivially satisfying the jump constraint ($\mathcal{X}_h^0 \subset \mathcal{X}_h$). We can now introduce the discrete approximation of problem (3.7):

Problem ($\mathbf{P}_h$): *find* $\mathbf{u}_h \in \mathcal{X}_h$ *such that for all* $\Phi_h \in \mathcal{X}_h$*:*

$$a_\tau(\mathbf{u}_h, \Phi_h) = (g, \Phi_h) \qquad \forall \Phi_h \in \mathcal{X}_h \tag{3.24}$$

Here g is different for different time discretizations.

We make the following typical assumptions on the spaces considered.

(A1) $\forall m = (\ell, i) \in I$ ($\gamma_\ell^{(i)}$ multiplier side), there exists a bounded projection $\pi_h^m : L^2(\gamma_m) \longrightarrow Y_h^{m,0}$, such that for all $\eta \in L^2(\gamma_m)$ and for all $\lambda \in M_h^m$

$$\int_{\gamma_m} (\eta - \pi_h^m \eta)\lambda \, ds = 0, \tag{3.25}$$

and for all $\eta \in H_{00}^{1/2}(\gamma_m)$

$$\|\pi_h^m \eta\|_{H_{00}^{1/2}(\gamma_m)} \lesssim \|\eta\|_{H_{00}^{1/2}(\gamma_m)}; \tag{3.26}$$

(A2) for all $\ell = 1, \ldots, L$, the following inverse inequalities hold: for all elements $\eta \in T_h^\ell$ and for all s, r $0 \le s < r \le 1$

$$|\eta|_{r,\Gamma_\ell} \lesssim h_\ell^{s-r} |\eta|_{s,\Gamma_\ell}, \tag{3.27}$$

$$|\eta|_{r,\gamma_\ell^{(i)}} \lesssim h_\ell^{s-r} |\eta|_{r,\gamma_\ell^{(i)}} \qquad i = 1, \ldots, 4; \tag{3.28}$$

(A3) $\forall \ell$ and $\forall \eta \in Y_h^\ell$ there exists a function $w_h \in \mathcal{V}_h^\ell$ such that

$$w_h = \eta \quad \text{ on } \Gamma_\ell, \qquad\qquad \|w_h\|_{1,\Omega_\ell} \lesssim \|\eta\|_{H^{1/2}(\Gamma_\ell)}. \tag{3.29}$$

By space interpolation, assumption (A.1) implies that the projection operator π_h^m verifies for all s, $0 < s < 1/2$:

$$\|\pi_h^m \eta\|_{H_0^s(\gamma_m)} \lesssim \|\eta\|_{H_0^s(\gamma_m)}, \tag{3.30}$$

uniformly in s. Following [5], we need to introduce a global linear operator

$$\pi_h : \prod_{\ell=1}^{L} L^2(\partial\Omega_\ell) \longrightarrow \prod_{\ell=1}^{L} L^2(\partial\Omega_\ell), \qquad \pi_h(\eta) = (\eta_\ell^*)_{\ell=1,\cdots,L} \tag{3.31}$$

defined as π_h^m applied to the jump of η on multiplier sides, and zero elsewhere, namely

$$\eta_\ell^*|_{\gamma_m} = \pi_h^m([\eta]|_{\gamma_m}), \quad m = (\ell, i) \in I \qquad \eta_\ell^*|_{\gamma_m} = 0, \quad m = (\ell, i) \in I^*. \tag{3.32}$$

Writing conventionally

$$\frac{H}{h} = \max_\ell \left\{ \frac{H_\ell}{h_\ell} \right\}, \tag{3.33}$$

the following property holds (see [5]):

$$\|\pi_h(\eta)\|_Y \lesssim \left(1 + \log \frac{H}{h}\right) \|\eta\|_Y. \tag{3.34}$$

If η is linear on each γ_ℓ^i the following improved estimate can be shown ([4]).

COROLLARY 3.4. *If assumptions (A1–A3) hold, then for any $\eta = (\eta_\ell)_{\ell=1,\cdots,L}$ in the trace space T such that η is linear on each $\gamma_\ell^{(i)}$, it holds that*

$$\|\pi_h(\eta)\|_Y \lesssim \left(1 + \log \frac{H}{h}\right)^{1/2} \|\eta\|_Y. \tag{3.35}$$

By using the nodal basis functions, equation (3.24) can be transformed into a large linear system of equations, that is usually not well conditioned. We now focus on preconditioners based on substructuring for solving the system at each time step.

4. Substructuring Preconditioners. In this section we propose a substructuring preconditioner, in terms of sums of bilinear forms, for the problem described in the previous section. A discrete counterpart will be deduced in section 6. We will consider the "substructuring" approach first introduced in [6] and already studied in the case of the Mortar Finite Element method in [1]. The principle of these preconditioners consists in distinguishing three types of degrees of freedom: *interior* degrees of freedom (corresponding to basis functions vanishing on the skeleton and supported on one sub-domain), *edge* degrees of freedom, and *vertex* degrees of freedom. This corresponds to splitting the functions $u \in \mathcal{X}_h$ as the sum of three suitably defined components: $u = u^0 + u^E + u^V$. A substructuring preconditioner conveniently exploits this splitting by approximating the bilinear form separately on each component space.

We next describe the operator splitting. Any discrete function $\boldsymbol{w} = (\boldsymbol{w}_\ell)_{\ell=1,\cdots,L} \in X_h$ can be uniquely split as the sum of an *interior* function $\boldsymbol{w}^0 \in \mathcal{X}_h^0$ and a discrete lifting, performed subdomain-wise of its trace $\boldsymbol{\eta}(\boldsymbol{w}) = (\boldsymbol{w}^\ell|_{\partial\Omega_\ell})_{\ell=1,\cdots,L}$ that, with some abuse of notation we denote by $\underline{R}_h(\boldsymbol{w})$ (rather than by the heavier notation $\underline{R}_h(\boldsymbol{\eta}(\boldsymbol{w}))$), i.e. we have:

$$\boldsymbol{w} = \boldsymbol{w}^0 + \underline{R}_h(\boldsymbol{w}), \qquad w^0 \in \mathcal{X}_h^0.$$

One possible choice for $\underline{R}_h$ is the discrete harmonic extension, that is $\underline{R}_h(\boldsymbol{w}) = (\underline{R}_h^\ell(\boldsymbol{w}_\ell))_{\ell=1,\ldots,L}$, with $\underline{R}_h^\ell(\boldsymbol{w}_\ell)$ the unique element in $\mathcal{V}_h^\ell \times \mathcal{V}_h^\ell$ satisfying

$$\underline{R}_h^\ell(\boldsymbol{w}_\ell) = \boldsymbol{w}_\ell \text{ on } \Gamma_\ell, \qquad a_{\tau,\ell}(\underline{R}_h^\ell(\boldsymbol{w}_\ell), \mathbf{v}_h^\ell) = 0, \quad \forall v_h \in \mathcal{V}_h^{\ell,0} \times \mathcal{V}_h^{\ell,0}. \tag{4.1}$$

In summary, we can write the constrained function space as a direct sum of an interior and a trace component, $\mathcal{X}_h = \mathcal{X}_h^0 \oplus \underline{R}_h(\mathcal{T}_h)$. Analogously, for the unconstrained space, $X_h = X_h^0 \oplus \underline{R}_h(T_h)$.

Therefore, it is not difficult to verify that the form a_τ in (3.6) satisfies

$$a_\tau(\boldsymbol{w}, \mathbf{v}) = a_\tau(\boldsymbol{w}^0, \mathbf{v}^0) + a_\tau(\underline{R}_h(\boldsymbol{w}), \underline{R}_h(\mathbf{v})) := a_\tau(\boldsymbol{w}^0, \mathbf{v}^0) + s_\tau(\boldsymbol{\eta}(\boldsymbol{w}), \boldsymbol{\eta}(\mathbf{v})),$$

where the *discrete Steklov-Poincaré* operator $s : T_h \times T_h \to \mathbb{R}$ is defined by

$$s_\tau(\boldsymbol{\xi}, \boldsymbol{\eta}) := \sum_\ell a_{\tau,\ell}(\underline{R}_h^\ell(\boldsymbol{\xi}), \underline{R}_h^\ell(\boldsymbol{\eta})). \tag{4.2}$$

REMARK 4.1. *If $\boldsymbol{\eta}$ satisfies the jump constraint, so does $\underline{R}_h(\boldsymbol{\eta})$. In other words, if $\boldsymbol{\eta} \in \mathcal{T}_h$ then $\underline{R}_h(\boldsymbol{\eta}) \in \mathcal{X}_h$.*

We also need the following lemma, whose proof essentially follows the one in [24] for a single parabolic equation, and it is therefore omitted.

LEMMA 4.1. *For all* $\boldsymbol{\eta} \in T_h$ *it holds that* $\|\underline{R}_h(\boldsymbol{\eta})\|_\tau \simeq \|\boldsymbol{\eta}\|_{T,\tau}$.

In the rest of this paper we focus on the problem of preconditioning the discrete Steklov-Poincaré operator s_τ, while we refer to existing literature for preconditioners for $a_\tau(\boldsymbol{w}^0, \mathbf{v}^0)$.

4.1. Splitting of the trace space. To construct a preconditioner for s_τ, we first observe that the space of constrained skeleton functions $\mathcal{T}_h$ can be further split as the sum of *vertex* and *edge* functions. If we introduce the space

$$\mathfrak{L} = \{(\eta_\ell)_{\ell=1,\cdots,L},\ \eta_\ell \text{ is linear on each edge of } \Omega_\ell\}, \qquad \mathfrak{L} \subset \prod_{\ell=1}^{L} H_*^{1/2}(\partial\Omega_\ell), \quad (4.3)$$

then the space of constrained *vertex* functions can be defined by

$$\mathcal{Y}_h^V = (Id - \pi_h)\mathfrak{L}. \quad (4.4)$$

In the following we make the (non-restrictive) assumption $\mathfrak{L} \subset \mathcal{Y}_h$, which yields $\mathcal{Y}_h^V \subset \mathcal{Y}_h$. We then introduce the space of constrained *edge* functions $\mathcal{Y}_h^E \subset \mathcal{Y}_h$ defined by

$$\mathcal{Y}_h^E = \{\eta = (\eta_\ell)_{\ell=1,\cdots,L} \in \mathcal{Y}_h,\ \eta_\ell(A) = 0,\ \forall \text{ vertex } A \text{ of } \Omega_\ell\} \quad (4.5)$$

from which it follows $\mathcal{Y}_h = \mathcal{Y}_h^V \oplus \mathcal{Y}_h^E$ and

$$\mathcal{T}_h = \mathcal{T}_h^V \oplus \mathcal{T}_h^E, \quad \text{with } \mathcal{T}_h^V = \mathcal{Y}_h^V \times \mathcal{Y}_h^V, \quad \mathcal{T}_h^E = \mathcal{Y}_h^E \times \mathcal{Y}_h^E. \quad (4.6)$$

Moreover it can be easily verified that a function in $\mathcal{T}_h^E$ is uniquely defined by its value on trace edges, the value on multiplier edges being forced by the constraint.

The edge bilinear form. The edge bilinear form that we consider is suggested by the norm $\|\cdot\|_{T,\tau}$ defined on T in (3.11). More specifically, we introduce a global edge block diagonal bilinear form $\hat{s}^E : \mathcal{T}_h^E \times \mathcal{T}_h^E \longrightarrow \mathbb{R}$

$$\hat{s}^E(\boldsymbol{\eta}^E, \boldsymbol{\xi}^E) = \tau^{1/2} p^E(\boldsymbol{\eta}^E, \boldsymbol{\xi}^E) + \tau b^E(\boldsymbol{\eta}^E, \boldsymbol{\xi}^E) \quad (4.7)$$

where the bilinear forms $p^E(\cdot,\cdot)$ and $b^E(\cdot,\cdot)$ are given as

$$p^E(\boldsymbol{\eta}, \boldsymbol{\eta}) = \sum_{m=(\ell,k)\in I^*} p_{\ell,k}(\boldsymbol{\eta}_\ell, \boldsymbol{\eta}_\ell) \quad (4.8)$$

$$b^E(\boldsymbol{\eta}, \boldsymbol{\eta}) = \sum_{m=(\ell,i)\in I^*} b^i_{\ell,k}(\eta^i_\ell, \eta^i_\ell) + b^e_{\ell,k}(\eta^e_\ell, \eta^e_\ell) \quad (4.9)$$

and $b^i_{\ell,k}, b^e_{\ell,k} : Y^0_{\ell,k} \times Y^0_{\ell,k} \times \to \mathbb{R}$, $p_{l,k} : T^0_{l,k} \times T^0_{l,k} \times \to \mathbb{R}$, defined for any trace side $\gamma_\ell^{(k)}$, $m = (\ell, k) \in I^*$ as

$$b^i_{\ell,k}(\eta^i, \eta^i) \simeq \|\eta^i_\ell\|^2_{H^{1/2}_{00}(\gamma_\ell^{(i)})} \qquad b^e_{\ell,k}(\eta^e, \eta^e) \simeq \|\eta^e_\ell\|^2_{H^{1/2}_{00}(\gamma_\ell^{(i)})} \quad (4.10)$$

$$p_{\ell,k}(\boldsymbol{\eta}_\ell, \boldsymbol{\eta}_\ell) \simeq \|\eta^i_\ell - \eta^e_\ell\|^2_{L^2(\gamma_\ell^{(k)})}. \quad (4.11)$$

REMARK 4.2. The bilinear form $b^E(\cdot,\cdot)$ is similar to the one used for elliptic problems (see, e.g., [4], [3]), while $p^E(\cdot,\cdot)$ is related to the parabolic structure of our problem. The presence of τ before b^E in (4.7) comes from the definition of the form a_τ, whereas $\tau^{1/2}$ before p^E stems from the norm $\|\cdot\|_{T,\tau}$, that is used in the proof of Theorem 4.2. The form (4.7) allows the edge block of the preconditioner to be easily implemented. Indeed, for b^E we can use the same efficient approximations proposed for elliptic problems (see, e.g., [6], [8], [28], [29]) whereas p^E simply requires to assemble a mass matrix for each master side of the decomposition, see Section 8 for details.

The vertex bilinear form. We next consider the approximation of the bilinear form corresponding to the vertex space $\mathcal{T}_h^V$. Note that this space depends both on the discretization of Ω into subdomains, as in conforming domain decomposition methods [6], as well as on the meshes in the different subdomains.

The natural choice is to introduce a vertex block diagonal global bilinear form

$$\hat{s}^V : \mathcal{T}_h^V \times \mathcal{T}_h^V \longrightarrow \mathbb{R} \qquad \text{such that} \qquad \hat{s}^V(\boldsymbol{\eta}^V, \boldsymbol{\eta}^V) \simeq s_\tau(\boldsymbol{\eta}^V, \boldsymbol{\eta}^V). \tag{4.12}$$

As suggested in [6, 1], the choice $\hat{s}^V(\boldsymbol{\eta}^V, \boldsymbol{\eta}^V) = s_\tau(\boldsymbol{\eta}^V, \boldsymbol{\eta}^V)$ provides a bilinear form whose matrix counterpart may be expensive to deal with, especially on fine grids, both in terms of storage requirements and computational costs. Therefore, we consider working with suitable alternatives on fixed coarse meshes. More specifically, we follow the approach proposed in [3] where a cheaper preconditioner is derived, observing that all the spaces $\mathcal{T}_h^V$ for different values of h depend on the same set of degrees of freedom (the values at the vertices of the Ω_ℓ's), and they are, therefore, isomorphic.

To describe such approach, for each ℓ we first choose an auxiliary discretization space $\mathcal{V}_\delta^\ell \subset H^1(\Omega_\ell) \cap C^0(\bar{\Omega}_\ell)$ with $\delta = \delta_\ell \geq h_\ell$, and for each $m = (\ell, i) \in I$ ($\gamma_m = \gamma_\ell^{(i)}$ multiplier edge) a corresponding auxiliary multiplier space $M_\delta^m \subset L^2(\gamma_m)$. The spaces X_δ, M_δ, and $\mathcal{X}_\delta$, as well as T_δ^ℓ, T_δ and $\mathcal{T}_\delta$ are constructed starting from the $\mathcal{V}_\delta^\ell$'s and the M_δ^m's in the same way as the spaces X_h, M_h, and $\mathcal{X}_h$, as well as T_h^ℓ, T_h and $\mathcal{T}_h$ are built from the $\mathcal{V}_h^\ell$'s and the M_h^m's, according to definitions similar to section 3.3.

We make on the spaces $\mathcal{V}_\delta^\ell$ and M_δ^m the same assumptions that we made on the spaces $\mathcal{V}_h^\ell$ and M_h^m. Analogously to π_h in (3.31), we can define the operator

$$\pi_\delta : \prod_{\ell=1}^{L} L^2(\partial\Omega_\ell) \longrightarrow \prod_{\ell=1}^{L} L^2(\partial\Omega_\ell),$$

that for $\eta = (\eta_\ell)_{\ell=1,\cdots,L}$, $\pi_\delta(\eta) = (\eta_\ell^*)_{\ell=1,\cdots,L}$ is defined on multiplier sides as π_δ^m applied to the jump of η, while it is set identically zero on trace sides and on the external boundary $\partial\Omega$:

$$\eta_\ell^*|_{\gamma_m} = \pi_\delta^m([\eta]|_{\gamma_m}), \quad m = (\ell, i) \in I \qquad \eta_\ell^*|_{\gamma_m} = 0, \quad m = (\ell, i) \in I^*.$$

Using the notation in (3.33) and Corollary 3.4 , we have

$$\|\pi_\delta(\eta)\|_Y \lesssim \left(1 + \log\frac{H}{\delta}\right) \|\eta\|_Y. \tag{4.13}$$

If in addition η is linear on each on each $\gamma_\ell^{(i)}$ then the bound can be improved to

$$\|\pi_\delta(\eta)\|_Y \lesssim \left(1 + \log\frac{H}{\delta}\right)^{1/2} \|\eta\|_Y. \tag{4.14}$$

As already observed, letting

$$\mathcal{Y}_\delta^V := (Id - \pi_\delta)\mathfrak{L}$$

the spaces $\mathcal{Y}_\delta^V$ and $\mathcal{Y}_h^V$ are isomorphic, though not necessarily uniformly with respect to h and δ. Let us write down the isomorphism explicitly. Let $L^\ell : C^0(\Gamma_\ell) \to \mathfrak{L}^\ell = \{\eta_\ell : \ \eta_\ell \ \text{ linear on each edge of } \Omega_\ell\}$ be defined by $L^\ell(\eta)$ with $L^\ell\eta(A_i) = \eta(A_i)$ for each vertex A_i of Ω_ℓ. We can assemble $L : \prod_\ell C^0(\Gamma_\ell) \to \mathfrak{L}$ as

$$L(\eta) = (L^\ell\eta_\ell)_\ell$$

and we then define $P_\delta : \prod_\ell C^0(\Gamma_\ell) \to \mathcal{Y}_\delta^V$ as

$$P_\delta = (Id - \pi_\delta)L.$$

It is not difficult to check that $\mathcal{Y}_\delta^V = P_\delta\mathcal{Y}_h^V$ and as before let $\mathcal{T}_\delta^V = \mathcal{Y}_\delta^V \times \mathcal{Y}_\delta^V$.

We can now define the vertex block of the preconditioner. For each subdomain Ω_ℓ let $\underline{R}_\delta^\ell : T_\delta^\ell \to \mathcal{V}_\delta^\ell \times \mathcal{V}_\delta^\ell$ denote the discrete harmonic lifting, that is $\underline{R}_\delta^\ell(\boldsymbol{\eta})$ is the unique element in $\mathcal{V}_\delta^\ell \times \mathcal{V}_\delta^\ell$ which verifies

$$\underline{R}_\delta^\ell\boldsymbol{\eta}|_{\partial\Omega_\ell} = \boldsymbol{\eta} \qquad \text{and} \qquad a_{\tau,\ell}(\underline{R}_\delta^\ell(\underline{P}_\delta\boldsymbol{\eta}), \boldsymbol{w}_h) = 0, \qquad \text{for all } \boldsymbol{w}_h \in \mathcal{V}_\delta^{\ell,0} \times \mathcal{V}_\delta^{\ell,0}$$

with $\underline{P}_\delta = P_\delta \times P_\delta$. Then we can assemble a global lifting operator $\underline{R}_\delta : T_h \to X_h$ as

$$\underline{R}_\delta(\boldsymbol{\eta}) = (\underline{R}_\delta^\ell\boldsymbol{\eta}_\ell)_{\ell=1,\cdots,L}$$

and define a vertex global block diagonal bilinear form $\hat{s}^V : T_h^V \times T_h^V \to \mathbb{R}$ as

$$\hat{s}^V(\boldsymbol{\eta}^V, \boldsymbol{\xi}^V) := \sum_\ell a_{\tau,\ell}(\underline{R}_\delta^\ell(\underline{P}_\delta\boldsymbol{\eta}^V), \underline{R}_\delta^\ell(\underline{P}_\delta\boldsymbol{\xi}^V)). \tag{4.15}$$

4.2. The preconditioner. Finally, we can introduce our preconditioner assembling the approximation to the Steklov-Poincarè bilinear form in (4.2). Let $\hat{s} : \mathcal{T}_h \times \mathcal{T}_h \longrightarrow \mathbb{R}$ be defined as

$$\hat{s}(\boldsymbol{\eta}, \boldsymbol{\xi}) = \hat{s}^V(\boldsymbol{\eta}^V, \boldsymbol{\xi}^V) + \hat{s}^E(\boldsymbol{\eta}^E, \boldsymbol{\xi}^E), \tag{4.16}$$

and we can state the main theorem of the paper.

THEOREM 4.2. *Let $\boldsymbol{\eta} \in \mathcal{T}_h$ then we have:*

$$\left(1 + \log\frac{H}{h}\right)^{-2} s_\tau(\boldsymbol{\eta}, \boldsymbol{\eta}) \lesssim \hat{s}(\boldsymbol{\eta}, \boldsymbol{\eta}) \lesssim \left(1 + \log\frac{H}{h}\right)^2 s_\tau(\boldsymbol{\eta}, \boldsymbol{\eta}). \tag{4.17}$$

Moreover, if the decomposition is geometrically conforming then for $\delta > h$

$$\left(\left(1 + \log\frac{H}{h}\right)\left(1 + \log\frac{H}{\delta}\right)\right)^{-1} s_\tau(\boldsymbol{\eta}, \boldsymbol{\eta}) \lesssim \hat{s}(\boldsymbol{\eta}, \boldsymbol{\eta}) \lesssim \left(1 + \log\frac{H}{h}\right)^2 s_\tau(\boldsymbol{\eta}, \boldsymbol{\eta}), \tag{4.18}$$

while if $\delta = h$

$$s_\tau(\boldsymbol{\eta}, \boldsymbol{\eta}) \lesssim \hat{s}(\boldsymbol{\eta}, \boldsymbol{\eta}) \lesssim \left(1 + \log\frac{H}{h}\right)^2 s_\tau(\boldsymbol{\eta}, \boldsymbol{\eta}). \tag{4.19}$$

The proof of Theorem 4.2 is included in section 5 and follows the abstract formulation proposed in [4, 3] for elliptic problems. We then generalize the abstract formulation of [4, 3] to our case.

REMARK 4.3. It is known that for elliptic problems, a factor $\frac{1}{H^2}$ appears in the estimate if (4.4) is not used for the vertex space. Analogously, in the parabolic case, one gets the extra factor $\frac{\tau}{H^2}$ and the convergence depends on the time step τ (see [6], [8], [14]). Numerical evidence is reported in Section 8.

The proof of theorem 4.2 follows essentially the guidelines of the proofs of the analogous results in [6, 1, 4, 3, 24]. In the next section we retrace, for the sake of completeness, the main steps of the proof in the framework of the abstract formulation considered in [24, 3, 4] that allows the extension to our degenerate parabolic system of equations.

5. Proof of Theorem 4.2. We start by proving the following lemma.

LEMMA 5.1. *For all constrained functions $\boldsymbol{\xi} \in \mathcal{T}_h$ it holds*

$$s_\tau(\boldsymbol{\xi}, \boldsymbol{\xi}) \simeq \|\boldsymbol{\xi}\|^2_{T,\tau}. \tag{5.1}$$

Proof. Let $\boldsymbol{\xi} \in \mathcal{T}_h$. From the definition of s_τ and applying Lemmas 3.2-4.1 we have

$$s_\tau(\boldsymbol{\xi}, \boldsymbol{\xi}) := \sum_\ell a_{\tau,\ell}(\underline{R}^\ell_h(\boldsymbol{\xi}), \underline{R}^\ell_h(\boldsymbol{\xi})) \lesssim \sum_\ell |a_{\tau,\ell}(\underline{R}^\ell_h(\boldsymbol{\xi}), \underline{R}^\ell_h(\boldsymbol{\xi})| \lesssim \|\underline{R}_h(\boldsymbol{\xi})\|^2_\tau \lesssim \|\boldsymbol{\xi}\|_{T,\tau}.$$

Similarly we can obtain the other inequality hence the thesis. □

In the following we will also use the following lemma.

LEMMA 5.2. [2, Lemma 3.1(i)] *Let assumption (A2) holds and let $\mathfrak{L} \in Y^\ell_h$, then the following bounds hold:*

(i) for all $\xi \in Y^\ell_h$ such that $\xi(P) = 0$ for some $P \in \gamma^{(i)}_\ell$ it holds

$$\|\xi\|^2_{L^\infty(\gamma^{(i)}_\ell)} \lesssim \left(1 + \log \frac{H}{h}\right) |\xi|^2_{1/2,\gamma^{(i)}_\ell}; \tag{5.2}$$

(ii) for all $\xi \in Y^\ell_h$, letting A_i and B_i denote the two extrema of the segment $\gamma^{(i)}_\ell$, we have

$$(\xi(A_i) - \xi(B_i))^2 \lesssim \left(1 + \log \frac{H}{h}\right) |\xi|^2_{H^{1/2}(\gamma^{(i)}_\ell)}; \tag{5.3}$$

(iii) for all $\xi \in T^0_{\ell,i}$ it holds

$$\|\xi\|^2_{H^{1/2}_{00}(\gamma^{(i)}_\ell)} \lesssim \left(1 + \log\left(\frac{H_\ell}{h_\ell}\right)\right)^2 |\xi|^2_{H^{1/2}(\gamma^{(i)}_\ell)}. \tag{5.4}$$

LEMMA 5.3. [4] *For all $\eta = (\eta_\ell)_{\ell=1,\cdots,L} \in \mathcal{Y}^E_h$ we have*

$$\|\eta\|^2_Y \lesssim \left(1 + \log \frac{H}{h}\right)^2 \sum_{(\ell,i)\in I^*} \|\eta_\ell\|^2_{H^{1/2}_{00}(\gamma^{(i)}_\ell)}. \tag{5.5}$$

We also need the following two results that generalize Lemmas 3.2, 3.4, 3.5 of [6] (see [4] for the proof).

LEMMA 5.4. *Let $\eta = (\eta_\ell)_\ell \in T_h$. Then it holds*

$$|L\eta|_Y^2 \lesssim \left(1 + \log \frac{H}{h}\right) |\eta|_Y^2. \tag{5.6}$$

LEMMA 5.5. *Let assumption (A2) hold, and let $\xi \in Y_h^\ell$, $\xi(A) = 0$ for all A vertex of Ω_ℓ. Let $\zeta_L \in H^{1/2}(\partial\Omega_\ell)$, ζ_L linear on each edge of Ω_ℓ. Then it holds*

$$\sum_{k=1}^{4} \|\xi\|^2_{H_{00}^{1/2}(\gamma_\ell^{(i)})} \lesssim \left(1 + \log \frac{H_\ell}{h_\ell}\right)^2 \|\xi + \zeta_L\|^2_{H^{1/2}(\partial\Omega_\ell)}. \tag{5.7}$$

We are now in a position to prove Theorem 4.2. Let us consider at first the non geometrically conforming case. Let $\boldsymbol{\eta} \in \mathcal{T}_h$, $\boldsymbol{\eta} = \boldsymbol{\eta}^V + \boldsymbol{\eta}^E$. By applying (5.1), (4.7), (5.5) and (4.12) we get

$$s_\tau(\boldsymbol{\eta}, \boldsymbol{\eta}) \lesssim |\boldsymbol{\eta}^E|_T^2 + |\boldsymbol{\eta}^V|_T^2 \lesssim \left(1 + \log \frac{H}{h}\right)^2 \hat{s}^E(\boldsymbol{\eta}^E, \boldsymbol{\eta}^E) + |\boldsymbol{\eta}^V|_T^2. \tag{5.8}$$

Now, using Lemma 5.4 and focusing on the component η^i of $\boldsymbol{\eta} = (\eta^i, \eta^e)$, since $(Id - \pi_\delta)L\eta^i \in \mathcal{Y}_\delta$ we can bound

$$\begin{aligned} |\eta_i^V|_Y^2 = |(Id - \pi_h)L\eta^i|_Y^2 &\lesssim \left(1 + \log \frac{H}{h}\right) |L\eta^i|_Y^2 \\ &= \left(1 + \log \frac{H}{h}\right) |L(Id - \pi_\delta)L\eta^i|_Y^2 \\ &\lesssim \left(1 + \log \frac{H}{h}\right)\left(1 + \log \frac{H}{\delta}\right) |(Id - \pi_\delta)L\eta^i|_Y^2. \end{aligned}$$

Since $\delta_\ell \geq h_\ell$ for all ℓ, we get $\log(H/\delta) \leq \log(H/h)$, so that, in view of the definition of $\hat{s}$ and of $\hat{s}^V$ (cf. (4.16)), we obtain

$$s_\tau(\boldsymbol{\eta}^V \boldsymbol{\eta}^V) \lesssim \left(1 + \log \frac{H}{h}\right)^2 \hat{s}(\boldsymbol{\eta}, \boldsymbol{\eta}).$$

On the other hand, for $\boldsymbol{\eta}^V = (\eta_i^V, \eta_e^V) \in \mathcal{T}_h^V$ we have

$$\begin{aligned} |(Id - \pi_\delta)L\eta^i|_Y^2 &\lesssim \left(1 + \log \frac{H}{\delta}\right) |L\eta^i|_Y^2 \\ &\lesssim \left(1 + \log \frac{H}{\delta}\right)\left(1 + \log \frac{H}{h}\right) |\eta^i|_Y^2 \end{aligned}$$

and from the definition of $\hat{s}^V$ we get $\hat{s}^V(\boldsymbol{\eta}^V, \boldsymbol{\eta}^V) \lesssim s_\tau(\boldsymbol{\eta}, \boldsymbol{\eta})$.

Let us now consider the second term in the sum at the right-hand side of (4.16). We have that $\hat{s}^E(\boldsymbol{\eta}^E, \boldsymbol{\eta}^E) = \sum_{m \in I^*} \|\eta_i^E\|^2_{H_{00}^{1/2}(\gamma_m)} + \|\eta_e^E\|^2_{H_{00}^{1/2}(\gamma_m)}$ and

$$\sum_{m \in I^*} \|\eta_i^E\|^2_{H_{00}^{1/2}(\gamma_m)} \lesssim \sum_{m \in I^*} \|\eta_i^E\|^2_{H_{00}^{1/2}(\gamma_m)} + \sum_{m \in I} \|\eta^i - L\eta^i\|^2_{H_{00}^{1/2}(\gamma_m)}.$$

We now observe that on "trace sides" ($m \in I^*$) we have $\eta_i^E = \eta^i - L\eta^i$. The same can be obtained for the extracellular component η^e, then we can apply lemma 5.5 getting

$$\hat{s}^E(\boldsymbol{\eta}^E, \boldsymbol{\eta}^E) \lesssim \left(1 + \log \frac{H}{h}\right)^2 s_\tau(\boldsymbol{\eta}, \boldsymbol{\eta}) \tag{5.9}$$

which, again in view of (4.16), concludes the proof of the first part of Theorem 4.2.

Let us now consider the geometrically conforming case. Once again, we have

$$s_\tau(\boldsymbol{\eta}, \boldsymbol{\eta}) \lesssim |\boldsymbol{\eta}^E|_T^2 + |\boldsymbol{\eta}^V|_T^2 \lesssim \left(1 + \log \frac{H}{h}\right)^2 \hat{s}^E(\boldsymbol{\eta}^E, \boldsymbol{\eta}^E) + |\boldsymbol{\eta}^V|_T^2. \tag{5.10}$$

Letting $\boldsymbol{\eta} = (\eta^i, \eta^e) \in \mathcal{T}_h^E$, and $\gamma_m = \Gamma_{\ell,\ell'}$ with ℓ master side and ℓ' slave side, we have

$$\|\eta^i_{\ell'}\|_{H_{00}^{1/2}(\gamma_m)} = \|\pi_m \eta^i_\ell\|_{H_{00}^{1/2}(\gamma_m)} \lesssim \|\eta^i_\ell\|_{H_{00}^{1/2}(\gamma_m)},$$

which implies

$$|\eta^i|_T = \sum_\ell |\eta^i_\ell|_{H^{1/2}(\Gamma_\ell)} = \sum_{(\ell,i)\in I\cup I^*} \|\eta_\ell\|_{H_{00}^{1/2}(\gamma_\ell^{(i)})} \lesssim \sum_{(\ell,i)\in I} \|\eta^i_\ell\|_{H_{00}^{1/2}(\gamma_\ell^{(i)})}.$$

Whence, $|\boldsymbol{\eta}^E|_T \lesssim b^E(\boldsymbol{\eta}^E, \boldsymbol{\eta}^E)$ and $\|\boldsymbol{\eta}^E\|_{T,\tau} \lesssim \hat{s}^E(\boldsymbol{\eta}^E, \boldsymbol{\eta}^E)$. By bounding $|\boldsymbol{\eta}^V|$ as in the geometrically non-conforming case, we obtain

$$s_\tau(\boldsymbol{\eta}, \boldsymbol{\eta}) \lesssim \left(1 + \log \frac{H}{h}\right)\left(1 + \log \frac{H}{\delta}\right) \hat{s}(\boldsymbol{\eta}, \boldsymbol{\eta}).$$

If $h = \delta$, we can further improve this estimate. Indeed, for $\boldsymbol{\eta}^V = (\eta_i^V, \eta_e^V)$ in such a case we have

$$|\eta_i^V|_Y^2 = |(Id - \pi_h)L\eta^i|_Y^2 = |(Id - \pi_\delta)L\eta^i|_Y^2,$$

which finally implies $s_\tau(\boldsymbol{\eta}, \boldsymbol{\eta}) \lesssim \hat{s}(\boldsymbol{\eta}, \boldsymbol{\eta})$.

6. Matrix form. In this section we derive the matrix form of the discrete Steklov-Poincaré operator s_τ. By using the nodal basis functions, equation (3.24) can be transformed in the following linear system of equations:

$$\mathcal{A} = \begin{bmatrix} M + \tau A_i & -M \\ -M & M + \tau A_e \end{bmatrix} \begin{bmatrix} \mathbf{u^i} \\ \mathbf{u^e} \end{bmatrix} = \begin{bmatrix} \mathbf{b}_1 \\ -\mathbf{b}_1 \end{bmatrix}, \quad \Leftrightarrow \quad \mathcal{A}\mathbf{u} = \mathbf{b} \tag{6.1}$$

where M is the mass matrix, A_i, A_e are the stiffness matrices associated to the discretization of $a_W^{i,e}$ defined in (3.2). Moreover, $\mathbf{u} = (\mathbf{u^i}, \mathbf{u^e})$, $\mathbf{b}_1 = \tau(M\,\mathbf{u} - \mathbf{i}(\mathbf{u}) + \mathbf{i}_a)$, $\mathbf{i}(\mathbf{u}) = M\mathbf{I}(\mathbf{u})$ with $\mathbf{I}(\mathbf{u}) = (I(v_1(t)), \ldots, I(v_n(t)))^T$ and $\mathbf{i}_a(t) = \left\{\int_\Omega I_{app}(t)\phi_j\, dx;\ j = 1, \ldots, n\right\}$.

It can be shown that the matrix $\mathcal{A}$ is positive semidefinite, see e.g. [26]. Moreover, $\mathcal{A}[\mathbf{e}; \mathbf{e}] = \mathbf{0}$ and the system is consistent, in that $\mathbf{b}$ has zero mean, that is $[\mathbf{e}^T, \mathbf{e}^T]\mathbf{b} = \mathbf{0}$, where $\mathbf{e}$ is the vector of all ones. We reorder the vector of unknowns as:

$$\mathbf{u} = \begin{pmatrix} \mathbf{u}_0 \\ \mathbf{u}_E \\ \mathbf{u}_V \\ \mathbf{u}_S \end{pmatrix} \begin{matrix} \}n_0 \\ \}n_E \\ \}n_V \\ \}n_S \end{matrix},$$

where n_E and n_S are the number of master and slave edge elements, respectively, while n_0 and n_V are the number of interior and vertex nodes, respectively. Moreover, $nnp := n_S+n_E+n_V+n_0$ is the total number of nodes, while $N_m := n_E+n_V+n_0$ is the number of *master* nodes. We emphasize that after this reordering, the intra and extra cellular potentials are ordered within each type of node, that is $\mathbf{u}_0^T = \left(\mathbf{u}_{i,0}^T, \mathbf{u}_{e,0}^T\right)$, $\mathbf{u}_E^T = \left(\mathbf{u}_{i,E}^T, \mathbf{u}_{e,E}^T\right)$ and so on. With this notation the matrices A and B associated to the discretization of a_X and b can be written as:

$$A = \begin{pmatrix} A_0 & A_{0E} & A_{0V} & A_{0S} \\ A_{0E}^T & A_E & A_{EV} & A_{ES} \\ A_{V0}^T & A_{EV}^T & A_V & A_{VS} \\ A_{S0}^T & A_{ES}^T & A_{VS}^T & A_S \end{pmatrix} \tag{6.2}$$

with

$$A_0 = \begin{pmatrix} A_0^i & 0 \\ 0 & A_0^e \end{pmatrix} \qquad A_0^s = \left\{a_W^s(\phi_k^0, \phi_\ell^0),\, k,l = 1,\dots,n_0\right\}, \quad s = i,e$$

and the other block matrices $A_{0E}, A_{0V}, A_{0S}, A_E, \dots$ defined analogously, and

$$B = \begin{pmatrix} B_0 & 0 & 0 & 0 \\ 0 & B_E & 0 & 0 \\ 0 & 0 & B_V & 0 \\ 0 & 0 & 0 & B_S \end{pmatrix}, \qquad B_s = \begin{pmatrix} M_s & -M_s \\ -M_s & M_s \end{pmatrix}, \quad s = 0,E,V,S. \tag{6.3}$$

Then, the system to be solved becomes

$$\mathcal{A}\mathbf{u} = \mathbf{b}, \tag{6.4}$$

with $\mathcal{A} = (B + \tau A)$ and $\mathbf{b}^T = (\mathbf{b}_0^T, \mathbf{b}_E^T, \mathbf{b}_V^T, \mathbf{b}_S^T)$.

Switching Matrix Q. From the mortar condition it follows that the interior nodes of the multiplier sides are not associated with genuine degrees of freedom in the FEM space. Indeed, the value of those coefficients corresponding to basis functions "living" on slave sides is uniquely determined by the remaining coefficients through the jump condition, and can be eliminated from the global vector $\mathbf{u}$. More precisely, the constrained coefficients $\mathbf{u}_S$ are uniquely determined through the mortar condition, i.e.

$$C_S\mathbf{u}_S = -C_E\mathbf{u}_E - C_V\mathbf{u}_V \qquad \begin{aligned}\mathbf{u}_S &= -C_S^{-1}C_E\mathbf{u}_E - C_S^{-1}C_V\mathbf{u}_V \\ &=: Q_E\mathbf{u}_E + Q_V\mathbf{u}_V\end{aligned} \tag{6.5}$$

where the entries of the mass matrices C_S, C_E, C_V are given by $c_{i,j} := \int_{\gamma_m}[\phi_j]\lambda_i\,ds$, $\lambda_i \in M_h$ and ϕ_j corresponding to the different nodal basis functions on the slave and master side and associated with the vertices. We note that C_S is a square matrix whereas C_E and C_V are rectangular matrices. Moreover, since we are using biorthogonal basis functions [33] C_S is a diagonal matrix hence C_S^{-1} can be easily computed.

Therefore, $\mathbf{u}_S$ can be eliminated thanks to a global "switching" matrix Q that also represents the constraint:

$$\mathbf{u} = Q\begin{pmatrix} \mathbf{u}_0 \\ \mathbf{u}_E \\ \mathbf{u}_V \end{pmatrix} \qquad \text{with} \qquad Q = \begin{pmatrix} I_0 & 0 & 0 \\ 0 & I_E & 0 \\ 0 & 0 & I_V \\ 0 & Q_E & Q_V \end{pmatrix}. \tag{6.6}$$

Therefore, in the system (6.4) the block of unknowns $\mathbf{u}_S$ can be eliminated by using the mortar condition, yielding the reduced system

$$\widetilde{\mathcal{A}}\mathbf{u}_M = \tilde{\mathbf{b}} \tag{6.7}$$

with $\widetilde{\mathcal{A}} = Q^T\mathcal{A}Q$ and $\tilde{\mathbf{b}} = Q^T\mathbf{b}$. More precisely, the new system may be viewed as the following block 3×3 system

$$\widetilde{\mathcal{A}} := \begin{pmatrix} K_{00} & K_{0E} & K_{0V} \\ K_{E0} & K_{EE} & K_{EV} \\ K_{V0} & K_{VE} & K_{VV} \end{pmatrix} \qquad \text{and} \qquad \tilde{\mathbf{b}} := \begin{pmatrix} \mathbf{b}_0 \\ \widetilde{\mathbf{b}}_E \\ \widetilde{\mathbf{b}}_V \end{pmatrix} \tag{6.8}$$

where $K_{00} = B_0 + \tau A_0$ and the other blocks are constructed according to the corresponding blocks of $\mathcal{A}$ and Q.

We note that the (1,1) block in $\widetilde{\mathcal{A}}$ is cheaply invertible (see also section 8), since it is associated with a Dirichlet problem in each subdomain. Therefore, the Schur complement of the system relative to the (1,1) block can readily be obtained, yielding the further reduced system

$$S = \begin{pmatrix} \mathbf{u}_E \\ \mathbf{u}_V \end{pmatrix} = \begin{pmatrix} \widehat{\mathbf{b}}_E \\ \widehat{\mathbf{b}}_V \end{pmatrix} \tag{6.9}$$

with

$$S = \begin{pmatrix} K_{EE} - K_{0E}^T K_{00}^{-1} K_{0E} & K_{EV} - K_{0E}^T K_{00}^{-1} K_{0V} \\ K_{EV}^T - K_{0V}^T K_{00}^{-1} K_{0E} & K_{VV} - K_{0V}^T K_{00}^{-1} K_{0V} \end{pmatrix} \tag{6.10}$$

and $\widehat{\mathbf{b}}_E = \widetilde{\mathbf{b}}_E - K_{0E}^T K_{00}^{-1}\mathbf{b}_0$, $\widehat{\mathbf{b}}_V = \widetilde{\mathbf{b}}_V - K_{0V}^T K_{00}^{-1}\mathbf{b}_0$. The Schur complement S represents the matrix form of the Steklov-Poincarè operator $s_\tau(\cdot,\cdot)$. However, the approximate bilinear form introduced in the previous section includes the splitting of the trace space given by (4.4)-(4.6), for which a discrete analogous can be obtained. To this end, we consider the space of linear functions $\mathfrak{L}$ defined in (4.3). Hence we introduce an interpolation map denoted by R_H^T (say piecewise interpolation) from the nodal value on V (vertices) onto all the nodes of $\mathcal{S}$. Consequently, R_H can be viewed as the weighted restriction map from $\mathcal{S}$ onto V. Then we define the square matrix

$$J = \begin{pmatrix} \begin{pmatrix} I_E \\ O \end{pmatrix} & R_H \end{pmatrix} \tag{6.11}$$

with I_E the identity matrix of size $n_E \times n_E$.

Let S be the matrix associated to the discrete Steklov–Poincaré operator $s_\tau(\cdot,\cdot)$ and $\widetilde{S}$ be the matrix obtained after applying the change of basis corresponding to switching from the standard nodal basis to the basis related to the splitting (4.4)-(4.6), that is

$$\widetilde{S} = J^T S J = \begin{pmatrix} \widetilde{S}_E & \widetilde{S}_{EV} \\ \widetilde{S}_{EV}^T & \widetilde{S}_V \end{pmatrix}. \tag{6.12}$$

Matrix $\widetilde{S}$ is the new Schur complement matrix, after applying the change of basis corresponding to the splitting (4.4)-(4.6). In the next section we describe a generalization of a known optimal preconditioner and some more computationally effective variants.

7. The preconditioner and its variants. Our preconditioner for $\widetilde{S}$ stems from the matrix discretization of the bilinear form $\hat{s}$, which yields the following diagonal (block-Jacobi type) preconditioner,

$$P = \begin{pmatrix} P_E & 0 \\ 0 & P_V \end{pmatrix}.$$

Note that P_E and P_V are the matrix counterparts of the bilinear forms $\hat{s}^E$ and $\hat{s}^V$, respectively (cf. (4.16)). The following result is an immediate consequence of Theorem 4.2 and shows the optimality of the preconditioner P.

COROLLARY 7.1. *Let $\widetilde{S}$ and P be the matrices obtained by discretizing respectively the bilinear forms s and $\hat{s}$. Then it holds*

$$\mathrm{Cond}(P^{-1}\widetilde{S}) \lesssim \left(1 + \log \frac{H}{h}\right)^4. \tag{7.1}$$

Moreover, if the decomposition is geometrically conforming then

$$\mathrm{Cond}(P^{-1}\widetilde{S}) \lesssim \left(1 + \log \frac{H}{h}\right)^3, \qquad \delta > h, \tag{7.2}$$

and

$$\mathrm{Cond}(P^{-1}\widetilde{S}) \lesssim \left(1 + \log \frac{H}{h}\right)^2, \qquad \delta = h. \tag{7.3}$$

We next describe three variants that make the preconditioner above computationally more appealing with no essential loss of optimality. This goal is achieved by replacing either or both the edge and vertex blocks P_E and P_V with more convenient approximations. In their construction, we were inspired by a similar approach first proposed in [6, 1, 4, 3] for elliptic problems.

The numerical tests in section 8 relate the three preconditioners P_1, P_2 and P_3 below, for the Schur complement system associated with the matrix in (6.12).

The preconditioner P_1. Following [6] and [1] for the mortar method, a simple approach consists in dropping all couplings between different edges and between edges and vertex points. More precisely, P_E is replaced by its block diagonal part

$$P_E^{diag} = \begin{pmatrix} P_{E_1,E_1} & 0 & 0 & 0 \\ 0 & P_{E_2,E_2} & 0 & 0 \\ 0 & 0 & \ddots & 0 \\ 0 & 0 & 0 & P_{E_m,E_m} \end{pmatrix}$$

with one block for each mortar where m is the number of mortars. This simplification provides our first variant,

$$P_1 = \begin{pmatrix} P_E^{diag} & 0 \\ 0 & P_V \end{pmatrix}.$$

The preconditioner P_2. A more efficient preconditioner may be obtained by using

(4.7), i.e. by approximating the edge block P_E of P as

$$P_E^{(R)} = \begin{pmatrix} \alpha\,\tau R^{1/2} + \beta\,\tau^{1/2}K & -\beta\,\tau^{1/2}K \\ -\beta\,\tau^{1/2}K & \alpha\,\tau R^{1/2} + \beta\,\tau^{1/2}K \end{pmatrix}$$
$$= \alpha\tau \begin{pmatrix} R^{1/2} & 0 \\ 0 & R^{1/2} \end{pmatrix} + \beta\,\tau^{1/2} \begin{pmatrix} K & -K \\ K & K \end{pmatrix} \equiv \alpha\,\tau R_E + \beta\,\tau^{1/2} K_E,$$

where R and K are $n_{E_i} \times n$ one dimensional Laplace and mass matrices, respectively, and α, β are suitably chosen parameters. In particular, they are related to the anisotropic conductivity tensors $M_{i,e}$ and can have a significant impact on the actual performance of the preconditioner. We next derive a result that will guide us in the choice of these two parameters. To emphasize the dependence on the parameters, we write the preconditioner $P_E^{(R)}$ as $P_E(\alpha, \beta)$. With this notation, we note that the matrix counterpart of the estimate (4.19) is given by

$$c_1(x, \widetilde{S}_E x) \le (x, P_E(1,1)x) \le c_2 \ell(x, \widetilde{S}_E x), \tag{7.4}$$

where c_1, c_2 are suitable constants that do not depend on h or H, but depend on $M_{i,e}$, while $\ell = (1 + \log(H/h))^2$.

PROPOSITION 7.2. *If $\alpha \ge c_1^{-1}$ and β is such that $\alpha \le \beta \le c_2^{-1}$ then*

$$(x, \widetilde{S}_E x) \le (x, P_E(\alpha, \beta)x) \le \ell(x, \widetilde{S}_E x).$$

Proof. On the one hand, for any nonzero vector x and for $\beta \ge \alpha$, it holds that $(x, P_E(\alpha,\beta)x) \ge \alpha(x, P_E(1,1)x) \ge \alpha c_1(x, \widetilde{S}_E x) \ge (x, \widetilde{S}_E x)$. On the other hand, $(x, P_E(\alpha,\beta)x) \le \beta(x, P_E(1,1)x) \le \beta c_2 \ell(x, \widetilde{S}_E x) \le \ell(x, \widetilde{S}_E x)$. ∎

In practice, the constants c_1, c_2 are not known exactly, however it can be seen that c_1 depends on $(\lambda_{\max}(M_{i,e}))^{-1}$, whereas, from (3.13), c_2 is related to $(\lambda_{\min}(M_{i,e}))^{-1/2}$. Therefore, without any further knowledge on the problem parameters, the proposition above suggests to take $\alpha \ge \lambda_{\max}(M_{i,e}) \approx 1/c_1$ and $\beta = (\lambda_{\min}(M_i))^{1/2} \approx 1/c_2$. In addition, numerical experiments showed that better performance was provided by an ever more refined selection of α, that is $\alpha_i \ge \lambda_{\max}(M_i)$ in the (1,1) block of $P_E^{(R)}$ and $\alpha_e \ge \lambda_{\max}(M_e)$ in the (2,2) block, yielding

$$P_E^{(R)} = \begin{pmatrix} \alpha_i\,\tau R^{1/2} + \beta\,\tau^{1/2}K & -\beta\,\tau^{1/2}K \\ -\beta\,\tau^{1/2}K & \alpha_e\,\tau R^{1/2} + \beta\,\tau^{1/2}K \end{pmatrix}.$$

This completely defines our second variant

$$P_2 = \begin{pmatrix} P_E^{(R)} & 0 \\ 0 & P_V \end{pmatrix}.$$

The preconditioner P_3. Our third variant stems from the already mentioned consideration that the vertex block P_V becomes expensive when grid refinements are required. We thus propose to approximate the vertex block P_V with the vertex preconditioner obtained with a fixed coarse mesh. Indeed, Theorem 4.2 and Corollary 7.1 ensure that we still have a polylogarithmic bound ($\left(1 + \log \frac{H}{h}\right)^3$ instead of $\left(1 + \log \frac{H}{h}\right)^2$ for the geometrically conforming decomposition). A key feature of this new vertex block preconditioner, called P_{Vc} in the sequel, is that it remains unchanged

if the mesh changes; this property is particularly appealing for parabolic problems, where the grid varies dynamically as time iterations proceed. Therefore, our third preconditioner is written as

$$P_3 = \begin{pmatrix} P_E^{(R)} & 0 \\ 0 & P_{Vc} \end{pmatrix}.$$

8. Numerical results. In this section we report our numerical experience with the preconditioners discussed in the previous section, when used in the Conjugate Gradient method. For simplicity we assume that each subdomain is rectangular and that the domain decomposition is geometrically conforming, i.e. the intersection of the closure of two subdomains is either empty, a vertex, or an entire common edge of the two subdomains. A uniform, geometrically conforming, domain decomposition of Ω into $K = N \times N$ equal square subdomains of size $H \times H$, is considered, with $H = 1/N$. In each subdomain Ω_k we take a uniform mesh $\mathcal{T}^k$ composed by $n_k \times n_k$ equal square elements of size $h_k \times h_k$, $h_k = H/n_k = 1/(Nn_k)$. In each subdomain Ω_k, we define V_h^k to be the space of Q_1 finite elements on the mesh $\mathcal{T}^k$:

$$V_h^k := \left\{ u_h \in C^0(\Omega_k) \,:\, u_{h_{|\tau}} \in Q_1(\tau),\, \forall \tau \in \mathcal{T}^k \right\}.$$

The multiplier space was chosen based on a dual basis, see [33].

The numerical tests relate the preconditioners for the Schur complement system defined in the previous sections as P_1, P_2 (with the first block defined in (7)) and P_3. To test the third preconditioner P_3, we generate the block P_{Vc} as the vertex block of the Schur complement discretized on an auxiliary coarse mesh.

Choice of the parameter for the anisotropic conductivity tensors $M_{i.e}$. The anisotropic conductivity tensors $M_s = \tilde{M}_s/c_m$ $s = i, e$ chosen for the numerical tests can be defined as:

$$\tilde{M}_s(\boldsymbol{x}) = \sigma_t^s I + (\sigma_l^s - \sigma_t^s)\ \mathbf{a}(\boldsymbol{x})\mathbf{a}(\boldsymbol{x})^T \qquad s = i, e \tag{8.1}$$

where c_m represents the surface capacitance of the membrane, $\mathbf{a} = \mathbf{a}(\boldsymbol{x})$ is the unit vector tangent to the cardiac fiber at a point $\boldsymbol{x} \in \Omega$, I is the identity matrix and σ_l^s, σ_t^s for $s = i, e$ are the conductivity coefficients along and across fiber, in the (i) and (e) media, assumed constant with $\sigma_l^s > \sigma_t^s > 0$. It can be easily verified that $M_{i,e}$ are symmetric positive definite matrices with two different distinct eigenvalues $\sigma_{l,t}^i$ and $\sigma_{l,t}^e$ respectively, both positive; the multiplicity of σ_l^s and σ_t^s for $s = i, e$ is 1 and 2, respectively, moreover,

$$\sigma_t^s |\boldsymbol{\xi}|^2 \le \boldsymbol{\xi}^T M_s(\boldsymbol{x}) \boldsymbol{\xi} \le \sigma_l^s |\boldsymbol{\xi}|^2 \qquad \forall \boldsymbol{\xi} \in \mathbf{R}^3, \boldsymbol{x} \in \Omega \quad s = i, e. \tag{8.2}$$

We considered the same parameter calibration used in [26] as reported in the table below.

$\chi = 1000$ cm^{-1}	$G = 4. \times 10^{-4}$ Ω^{-1} cm^{-2}	$c_m = 0.8\mu F$ cm^{-2}
$i_{app} = 0.8$ A cm^{-3}	$v_p = 100$ mV	$v_{th} = 10$ mV
$\sigma_l^e = 2.5 \times 10^{-3}$,	$\sigma_t^e = 1.25 \times 10^{-3}$	Ω^{-1} cm^{-1}
$\sigma_l^i = 2. \times 10^{-3}$,	$\sigma_t^i = 4.16 \times 10^{-4}$	Ω^{-1} cm^{-1}

with $I_{app} = \frac{\chi}{c_m} i_{app}$. Other definitions of $M_{i,e}$ and/or of the coefficients $\sigma_{l,t}^{i,e}$ can be found in literature (see, e.g., [10]) but our theory can be easily extended to these different cases.

As already stated in the construction of P_2, suitable constants related to $M_{i,e}$ need to be introduced. Proposition 7.2, the subsequent discussion and numerical experiments suggest to take the following values for α_i, α_e and β:

$$\alpha_i = \frac{2\sigma_t^i + \sigma_l^i}{c_m} \geq \lambda_{\max}(M_i), \quad \alpha_e = \frac{2\sigma_t^e + \sigma_l^e}{c_m} \geq \lambda_{\max}(M_e),$$
$$\beta = \left(\frac{\sigma_t^i}{c_m}\right)^{1/2} = (\lambda_{\min}(M_i))^{1/2}.$$

Conforming decomposition. To validate our theory we start by considering a conforming decomposition, i.e. we set $n_k = n$ for all k. In this case $h_k = h = H/n$ and we obtain the same solution that we would get using a conforming finite element method on a regular grid of $Nn \times Nn$ square elements of dimension $h \times h$ each. To study the dependence on h and on the size of the subdomains H, we considered several combinations of N and n with $n \in \{5, 6, \ldots, 50\}$ and $N \in \{4, 5, \ldots, 32\}$. We remark that in this special case, $\max_k H_k/h_k = H/h = n$.

Table 8.1 shows the number of PCG iterations to reduce the residual of a factor 10^{-5} with the preconditioners P_1, P_2 and P_3. The coarse auxiliary mesh of P_3 is obtained by considering a uniform mesh in each subdomain made up of 5×5 elements. For comparison purposes and to highlight the importance of the choice of the parameters $\alpha_i, \alpha_e, \beta$ we also report the significantly higher number of iterations required by preconditioner P_2 when $\alpha_i = \alpha_e = \beta = 1$. The results are in close agreement with the theory: the number of PCG iterations grows at most polylogarithmically with the number of degrees of freedom per subdomain, as indicated by (7.3).

	P_1			P_2			P_3			$P_2(1,1)$		
$N^2 \backslash n$	5	10	20	5	10	20	5	10	20	5	10	20
16	32	45	55	45	49	54	45	61	74	56	61	75
64	31	41	51	38	43	50	38	46	59	42	53	69
144	30	36	42	33	39	44	33	42	49	40	51	53
256	28	33	36	30	38	43	30	40	43	40	50	55
400	28	32	35	30	36	40	30	37	42	42	52	61
576	25	28	32	27	35	39	27	36	41	45	55	61
784	24	28	32	28	35	39	28	36	40	49	56	61

TABLE 8.1

Number of PCG iterations for preconditioners P_1, P_2, P_3 for different combinations of the number $K = N^2$ of subdomains and n elements per edge (n^2 elements per subdomains). The last column refers to preconditioner P_2 for $\alpha_i = \alpha_e = \beta = 1$.

Non-conforming decomposition. We next study a nonconforming decomposition. We consider two test configurations, both based on a decomposition of Ω into 5×5 subdomains. In the first case (left plot of Figure 8.1), in all but two subdomains we set $n_k = 10$. In the remaining two subdomains we set $n_k = n$ with n in $\{10, \ldots, 52\}$. In the second configuration (center plot of Figure 8.1) we set again $n_k = 10$ in all domains except a 3×3 block of subdomains, where $n_k = n$, with n as before.

The results for both configurations and all three preconditioners are reported in Table 8.2. In this case the coarse auxiliary mesh for P_3 is obtained by considering a uniform mesh in each subdomain made up of 10×10 elements.

The theoretical estimates on the condition number only depend on $\max H_k/h_k$ and take similar values for both configurations. Again, we can conclude that the

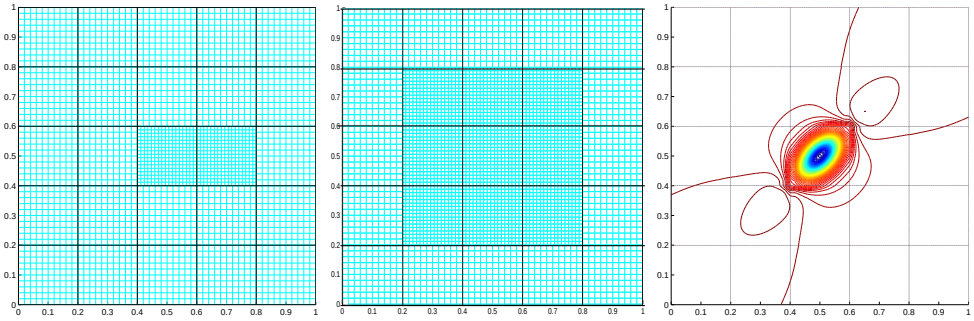

FIG. 8.1. *Splitting of* Ω *into* 5×5 *subdomains. Configuration 1 (left): for all subdomains we set* $n_k = 10$ *except two (# 13 and 14) where* $n_k = n$ *with* n *in the set* $\{10, \ldots, 52\}$. *Configuration 2 (center and right): we set again* $n_k = 10$, *except in a* 3×3 *block of subdomains where* $n_k = n$ *and* n *in* $\{10, \ldots, 52\}$. *Right: extracellular potential map computed with the mesh of configuration 2.*

	Configuration 1 Figure 8.1(left)			Configuration 2 Figure 8.1(center)		
n	P_1	P_2	P_3	P_1	P_2	P_3
10	44	45	45	44	45	45
17	57	59	60	58	57	62
24	65	66	71	64	67	71
31	66	69	75	69	71	78
38	72	74	78	71	74	82
45	72	77	82	73	76	83
52	73	77	80	73	76	87

TABLE 8.2

FEM. Number of PCG iterations for preconditioners P_1, P_2, *and* P_3 *when* $N = 5$ *and for different combinations of the number* n *of elements per edge* (n^2 *elements per subdomains).*

results are in close agreement with the theory, reporting at most polylogarithmical growth in the number of iterations, with respect to the number of degrees of freedom per subdomain. No relevant differences can be seen in Table 8.2 when using preconditioners P_1 and P_2. However, we recall that using P_2, and thus P_3, is significantly cheaper, both in terms of computational costs and memory requirements, than using P_1.

In summary, our numerical experiments with Q_1 finite elements confirm that an efficient variant of the vertex block proposed in [3] can be derived, yielding a cheaper and easier to implement preconditioner, without sacrificing the theoretical properties of the original substructuring technique (cf. Theorem 4.2 and Corollary 7.1). It is also remarkable that an appropriate selection of the parameters related to the conductivity tensors significantly improves the performance of the structured preconditioner.

8.1. Performance without (4.4) for the vertex space. In this section we experimentally analyze the dependence of the preconditioner on τ/H^2 when (4.4) is not used for the vertex space, that is when the matrix S is used instead of $\widetilde{S}$ (see Remark 4.3).

We consider once again the conforming decomposition and we perform numerical tests keeping fixed the mesh in each subdomain ($n = 5$) and varying the number of subdomains, i.e. H. More specifically we consider $H \in [4, 8, \ldots, 32]$ and $\tau \in$

$\{4.10^{-1}, 4.10^{-2}, 4.10^{-3}, 4.10^{-4}\}$. Note that $\tau = 4.10^{-2}$ is a time step typically used for simulations (see, e.g., [11, 26, 12]) whereas the other values of τ are considered only for comparison purposes.

Table 8.3 shows the number of PCG iterations required to reduce the residual of a factor of 10^{-5}. We report the results with P_1 and with the corresponding one obtained with no vertex correction, named P_1^{no}. he numbers indicate a clear dependence of the performance on the number of subdomains when no vertex correction is employed. This is true for all cases, except when the ratio τ/H^2 is very small (for the less common value $\tau = 4.10^{-4}$, hence $\tau/H^2 \in [2.5\,10^{-5}, \ldots, 5.1\,10^{-7}]$), in which case the results are comparable to those using vertex correction (cf. Remark 4.3).

τ	$4 \cdot 10^{-1}$		$4 \cdot 10^{-2}$		$4 \cdot 10^{-3}$		$4 \cdot 10^{-4}$	
N^2	P_1^{no}	P_1	P_1^{no}	P_1	P_1^{no}	P_1	P_1^{no}	P_1
4	15	30	13	32	12	33	10	35
64	30	27	26	30	21	30	13	33
144	45	26	39	30	29	30	16	32
256	62	25	52	28	40	29	16	30
400	78	25	64	28	49	29	23	30
576	94	26	78	25	60	29	26	29
784	110	25	89	24	70	28	26	29

TABLE 8.3

Number of PCG iterations for preconditioners P_1 and P_1^{no} (no vertex correction) for different combinations of the number $K = N^2$ of subdomains and $n = 5$ elements per edge.

Acknowledgments. The authors thank Giuseppe Savaré and Silvia Bertoluzza for helpful discussions. This work was partially supported by the IHP Project *Breaking Complexity*, contract HPRN-CT-2002-00286.

REFERENCES

[1] Y. Achdou, Y. Maday, and O. B. Widlund. Iterative substructuring preconditioners for mortar element methods in two dimensions. *SIAM J. Numer. Anal.*, 36(2):551–580, 1999.

[2] S. Bertoluzza. Substructuring preconditioners for the three fields domain decomposition method. *Math. Comp.*, 246(73):659–689, 2004.

[3] S. Bertoluzza and M. Pennacchio. Preconditioning the mortar method by substructuring: the high order case. *Appl. Num. Anal. Comp. Math.*, 1(3):434–454, 2004.

[4] S. Bertoluzza and M. Pennacchio. Analysis of substructuring preconditioners for mortar methods in an abstract framework. *to appear on Appl. Math. Lett.*, 2006.

[5] S. Bertoluzza and V. Perrier. The mortar method in the wavelet context. *ESAIM:M2AN*, 35:647–673, 2001.

[6] J. H. Bramble, J. E. Pasciak, and A. H. Schatz. The construction of preconditioners for elliptic problems by substructuring, I. *Math. Comp.*, 47(175):103–134, 1986.

[7] S. Brenner and R. Scott. *The mathematical theory of finite element methods.*, volume 15 of *Texts in Applied Mathematics*. Springer-Verlag, New York, second edition, 2002.

[8] T. F. Chan and T. P. Mathew. Domain decomposition algorithms. In *Acta Numerica 1994*, pages 61–143. Cambridge University Press, 1994.

[9] E. Cherry, H. Greenside, and C.H. Henriquez. Efficient simulation of three-dimensional anisotropic cardiac tissue using an adaptive mesh refinement method. *Chaos*, 3:853–865, 2003.

[10] P. Colli Franzone, P. Deuflhard, B. Erdmann, J. Lang, and L. Pavarino. Adaptivity in space and time for reaction-diffusion systems in electrocardiology. *to appear on SIAM J. Sci. Comput.*, 2005.

[11] P. Colli Franzone and L. Guerri. Spreading of excitation in 3-D models of the anisotropic cardiac tissue. I: Validation of the eikonal model. *Math. Biosci.*, 113:145–209, 1993.

[12] P. Colli Franzone and L. Pavarino. A parallel solver for reaction-diffusion systems in computational electrocardiology. *Math. Models Methods Appl. Sci.*, 14(6):883–911, 2004.

[13] P. Colli Franzone and G. Savaré. Degenerate evolution systems modeling the cardiac electric field at micro and macroscopic level. In *Evolution equations, Semigroups and Functional Analysis, Progr. Nonlinear Differential Equations Appl.*, volume 50, pages 49–78. Birkhauser, Basel, 2002.

[14] M. Dryja. Substructuring methods for parabolic problems. In *Proceedings of the Fourth International Symposium on Domain Decomposition Methods for Partial Differential Equations*, pages 264–271. SIAM, Philadelphia, 1991.

[15] C Henriquez, A Muzikant, and Smoak C. Anisotropy, fiber curvature, and bath loading effects on activation in thin and thick cardiac tissue preparations: Simulations in a three–dimensional bidomain model. *J. Cardiovasc. Electrophysiol.*, 7:424–444, 1996.

[16] C. S. Henriquez. Simulating the electrical behavior of cardiac tissue using the bidomain model. *Crit. Rev. Biomed. Engr.*, 21:1–77, 1993.

[17] N. Hooke, C. S. Henriquez, P. Lanzkron, and D. Rose. Linear algebraic transformations of the bidomain equations: implications for numerical methods. *Math. Biosci.*, 120:127–145, 1994.

[18] J. Keener and K. Bogar. A numerical method for the solution of the bidomain equations in cardiac tissue. *Chaos*, pages 234–241, 1998.

[19] G. T. Lines, M. L. Buist, P. Grøttum, and A. Tveito. Modeling the electrical activity of the heart: a bidomain model of the ventricles embedded in a torso. *Comput. Vis. Sci.*, 5(4):195–213, 2003.

[20] J. L. Lions and E. Magenes. *Non-Homogeneous Boundary Value Problems and Applications*. Springer-Verlag, 1972.

[21] C. Luo and Y. Rudy. A model of ventricular cardiac action potential: depolarization, repolarization, and their interaction. *Circ. Res.*, 68:1501–1526, 1991.

[22] M. Pennacchio. The mortar finite element method for cardiac reaction-diffusion models. In *Computers in Cardiology*, volume 31, pages 509–512. IEEE, 2004.

[23] M. Pennacchio. The mortar finite element method for the cardiac "bidomain" model of extracellular potential. *J. Sci. Comput.*, 20(2):191–210, 2004.

[24] M. Pennacchio. Substructuring preconditioners for mortar discretization of parabolic problems. Technical Report 1, IMATI-PV CNR, 2006.

[25] M. Pennacchio, G. Savaré, and P. Colli Franzone. Multiscale modeling for the bioelectric activity of the heart. *SIAM J. Math. Anal.*, 37(4):1333–1370, 2006.

[26] M. Pennacchio and V. Simoncini. Efficient algebraic solution of reaction-diffusion systems for the cardiac excitation process. *J. Comput. Appl. Math.*, 145(1):49–70, 2002.

[27] J. B. Pormann. *A modular simulation system for the bidomain equations*. PhD thesis, Dept. of Electrical and Computer Engineering, Duke University, 1999.

[28] B. F. Smith, P. E. Bjorstad, and W. D. Gropp. *Parallel multilevel methods for partial differential equations*. Cambridge University Press, 1986.

[29] A. Toselli and O. Widlund. *Domain Decomposition Methods - Algorithms and Theory*, volume 34 of *Springer Series in Computational Mathematics*. Springer, 2004.

[30] J. A. Trangestein and C. Kim. Operator splitting and adaptive mesh refinement for the luo-rudy I model. *J. Computational Physics*, 196:645–679, 2004.

[31] H. Triebel. *The structure of functions*. Birkhäuser, 2001.

[32] R. Weber Dos Santos, G. Plank, S. Bauer, and E. Vigmond. Parallel multigrid preconditioner for the cardiac bidomain model. *IEEE Transactions on Biomedical Engeneering*, 51:1960–1968, 2004.

[33] B. Wohlmuth. *Discretization Methods and Iterative Solvers Based on Domain Decomposition*, volume 17 of *Lecture Notes in Computational Science and Engineering*. Springer, 2001.